

BNL-52627, CLNS 01/1729, FERMILAB-Pub-01/058-E,
LBNL-47813, SLAC-R-570, UCRL-ID-143810-DR
LC-REV-2001-074-US
hep-ex/0106055
June 2001

Linear Collider Physics Resource Book for Snowmass 2001

Part 1: Introduction

American Linear Collider Working Group *

Abstract

This Resource Book reviews the physics opportunities of a next-generation e^+e^- linear collider and discusses options for the experimental program. Part 1 contains the table of contents and introduction and gives a summary of the case for a 500 GeV linear collider.

*Work supported in part by the US Department of Energy under contracts DE-AC02-76CH03000, DE-AC02-98CH10886, DE-AC03-76SF00098, DE-AC03-76SF00515, and W-7405-ENG-048, and by the National Science Foundation under contract PHY-9809799.

**Linear Collider
Physics
Resource Book
for
Snowmass 2001**

American Linear Collider
Working Group

BNL-52627, CLNS 01/1729, FERMILAB-Pub-01/058-E,
LBNL-47813, SLAC-R-570, UCRL-ID-143810-DR

LC-REV-2001-074-US

June 2001

This document, and the material and data contained therein, was developed under sponsorship of the United States Government. Neither the United States nor the Department of Energy, nor the Leland Stanford Junior University, nor their employees, nor their respective contractors, subcontractors, or their employees, makes any warranty, express or implied, or assumes any liability of responsibility for accuracy, completeness or usefulness of any information, apparatus, product or process disclosed, or represents that its use will not infringe privately owned rights. Mention of any product, its manufacturer, or suppliers shall not, nor is intended to imply approval, disapproval, or fitness for any particular use. A royalty-free, nonexclusive right to use and disseminate same for any purpose whatsoever, is expressly reserved to the United States and the University.

Cover: Events of $e^+e^- \rightarrow Z^0 h^0$, simulated with the Large linear collider detector described in Chapter 15. Front cover: $h^0 \rightarrow \tau^+\tau^-$, $Z^0 \rightarrow b\bar{b}$. Back cover: $h^0 \rightarrow b\bar{b}$, $Z^0 \rightarrow \mu^+\mu^-$.

Typset in L^AT_EX by S. Jensen.

Prepared for the Department of Energy under contract number DE-AC03-76SF00515 by Stanford Linear Accelerator Center, Stanford University, Stanford, California. Printed in the United State of America. Available from National Technical Information Services, US Department of Commerce, 5285 Port Royal Road, Springfield, Virginia 22161.

American Linear Collider Working Group

T. Abe⁵², N. Arkani-Hamed²⁹, D. Asner³⁰, H. Baer²², J. Bagger²⁶, C. Balazs²³,
C. Baltay⁵⁹, T. Barker¹⁶, T. Barklow⁵², J. Barron¹⁶, U. Baur³⁸, R. Beach³⁰,
R. Bellwied⁵⁷, I. Bigi⁴¹, C. Blöching⁵⁸, S. Boege⁴⁷, T. Bolton²⁷, G. Bower⁵²,
J. Brau⁴², M. Breidenbach⁵², S. J. Brodsky⁵², D. Burke⁵², P. Burrows⁴³,
J. N. Butler²¹, D. Chakraborty⁴⁰, H. C. Cheng¹⁴, M. Chertok⁶, S. Y. Choi¹⁵,
D. Cinabro⁵⁷, G. Corcella⁵⁰, R. K. Cordero¹⁶, N. Danielson¹⁶, H. Davoudiasl⁵²,
S. Dawson⁴, A. Denner⁴⁴, P. Derwent²¹, M. A. Diaz¹², M. Dima¹⁶, S. Dittmaier¹⁸,
M. Dixit¹¹, L. Dixon⁵², B. Dobrescu⁵⁹, M. A. Doncheski⁴⁶, M. Duckwitz¹⁶,
J. Dunn¹⁶, J. Early³⁰, J. Erler⁴⁵, J. L. Feng³⁵, C. Ferretti³⁷, H. E. Fisk²¹, H. Fraas⁵⁸,
A. Freitas¹⁸, R. Frey⁴², D. Gerdes³⁷, L. Gibbons¹⁷, R. Godbole²⁴, S. Godfrey¹¹,
E. Goodman¹⁶, S. Gopalakrishna²⁹, N. Graf⁵², P. D. Grannis³⁹, J. Gronberg³⁰,
J. Gunion⁶, H. E. Haber⁹, T. Han⁵⁵, R. Hawkings¹³, C. Hearty³, S. Heinemeyer⁴,
S. S. Hertzbach³⁴, C. Heusch⁹, J. Hewett⁵², K. Hikasa⁵⁴, G. Hiller⁵², A. Hoang³⁶,
R. Hollebeek⁴⁵, M. Iwasaki⁴², R. Jacobsen²⁹, J. Jaros⁵², A. Juste²¹, J. Kadyk²⁹,
J. Kalinowski⁵⁷, P. Kalyniak¹¹, T. Kamon⁵³, D. Karlen¹¹, L. Keller⁵², D. Koltick⁴⁸,
G. Kribs⁵⁵, A. Kronfeld²¹, A. Leike³², H. E. Logan²¹, J. Lykken²¹, C. Macesanu⁵⁰,
S. Magill¹, W. Marciano⁴, T. W. Markiewicz⁵², S. Martin⁴⁰, T. Maruyama⁵²,
K. Matchev¹³, K. Moenig¹⁹, H. E. Montgomery²¹, G. Moortgat-Pick¹⁸, G. Moreau³³,
S. Mrenna⁶, B. Murakami⁶, H. Murayama²⁹, U. Nauenberg¹⁶, H. Neal⁵⁹,
B. Newman¹⁶, M. Nojiri²⁸, L. H. Orr⁵⁰, F. Paige⁴, A. Para²¹, S. Pathak⁴⁵,
M. E. Peskin⁵², T. Plehn⁵⁵, F. Porter¹⁰, C. Potter⁴², C. Prescott⁵², D. Rainwater²¹,
T. Raubenheimer⁵², J. Repond¹, K. Riles³⁷, T. Rizzo⁵², M. Ronan²⁹,
L. Rosenberg³⁵, J. Rosner¹⁴, M. Roth³¹, P. Rowson⁵², B. Schumm⁹, L. Seppala³⁰,
A. Seryi⁵², J. Siegrist²⁹, N. Sinev⁴², K. Skulina³⁰, K. L. Sterner⁴⁵, I. Stewart⁸,
S. Su¹⁰, X. Tata²³, V. Telnov⁵, T. Teubner⁴⁹, S. Tkaczyk²¹, A. S. Turcot⁴,
K. van Bibber³⁰, R. van Kooten²⁵, R. Vega⁵¹, D. Wackerroth⁵⁰, D. Wagner¹⁶,
A. Waite⁵², W. Walkowiak⁹, G. Weiglein¹³, J. D. Wells⁶, W. Wester, III²¹,
B. Williams¹⁶, G. Wilson¹³, R. Wilson², D. Winn²⁰, M. Woods⁵², J. Wudka⁷,
O. Yakovlev³⁷, H. Yamamoto²³, H. J. Yang³⁷

- ¹ Argonne National Laboratory, Argonne, IL 60439
- ² Universitat Autònoma de Barcelona, E-08193 Bellaterra, Spain
- ³ University of British Columbia, Vancouver, BC V6T 1Z1, Canada
- ⁴ Brookhaven National Laboratory, Upton, NY 11973
- ⁵ Budker INP, RU-630090 Novosibirsk, Russia
- ⁶ University of California, Davis, CA 95616
- ⁷ University of California, Riverside, CA 92521
- ⁸ University of California at San Diego, La Jolla, CA 92093
- ⁹ University of California, Santa Cruz, CA 95064
- ¹⁰ California Institute of Technology, Pasadena, CA 91125
- ¹¹ Carleton University, Ottawa, ON K1S 5B6, Canada
- ¹² Universidad Católica de Chile, Chile
- ¹³ CERN, CH-1211 Geneva 23, Switzerland
- ¹⁴ University of Chicago, Chicago, IL 60637
- ¹⁵ Chonbuk National University, Chonju 561-756, Korea
- ¹⁶ University of Colorado, Boulder, CO 80309
- ¹⁷ Cornell University, Ithaca, NY 14853
- ¹⁸ DESY, D-22063 Hamburg, Germany
- ¹⁹ DESY, D-15738 Zeuthen, Germany
- ²⁰ Fairfield University, Fairfield, CT 06430
- ²¹ Fermi National Accelerator Laboratory, Batavia, IL 60510
- ²² Florida State University, Tallahassee, FL 32306
- ²³ University of Hawaii, Honolulu, HI 96822
- ²⁴ Indian Institute of Science, Bangalore, 560 012, India
- ²⁵ Indiana University, Bloomington, IN 47405
- ²⁶ Johns Hopkins University, Baltimore, MD 21218
- ²⁷ Kansas State University, Manhattan, KS 66506
- ²⁸ Kyoto University, Kyoto 606, Japan
- ²⁹ Lawrence Berkeley National Laboratory, Berkeley, CA 94720
- ³⁰ Lawrence Livermore National Laboratory, Livermore, CA 94551
- ³¹ Universität Leipzig, D-04109 Leipzig, Germany
- ³² Ludwigs-Maximilians-Universität, München, Germany
- ^{32a} Manchester University, Manchester M13 9PL, UK
- ³³ Centre de Physique Théorique, CNRS, F-13288 Marseille, France
- ³⁴ University of Massachusetts, Amherst, MA 01003
- ³⁵ Massachusetts Institute of Technology, Cambridge, MA 02139
- ³⁶ Max-Planck-Institut für Physik, München, Germany
- ³⁷ University of Michigan, Ann Arbor MI 48109
- ³⁸ State University of New York, Buffalo, NY 14260
- ³⁹ State University of New York, Stony Brook, NY 11794
- ⁴⁰ Northern Illinois University, DeKalb, IL 60115

- ⁴¹ University of Notre Dame, Notre Dame, IN 46556
- ⁴² University of Oregon, Eugene, OR 97403
- ⁴³ Oxford University, Oxford OX1 3RH, UK
- ⁴⁴ Paul Scherrer Institut, CH-5232 Villigen PSI, Switzerland
- ⁴⁵ University of Pennsylvania, Philadelphia, PA 19104
- ⁴⁶ Pennsylvania State University, Mont Alto, PA 17237
- ⁴⁷ Perkins-Elmer Bioscience, Foster City, CA 94404
- ⁴⁸ Purdue University, West Lafayette, IN 47907
- ⁴⁹ RWTH Aachen, D-52056 Aachen, Germany
- ⁵⁰ University of Rochester, Rochester, NY 14627
- ⁵¹ Southern Methodist University, Dallas, TX 75275
- ⁵² Stanford Linear Accelerator Center, Stanford, CA 94309
- ⁵³ Texas A&M University, College Station, TX 77843
- ⁵⁴ Tokoku University, Sendai 980, Japan
- ⁵⁵ University of Wisconsin, Madison, WI 53706
- ⁵⁷ Uniwersytet Warszawski, 00681 Warsaw, Poland
- ⁵⁷ Wayne State University, Detroit, MI 48202
- ⁵⁸ Universität Würzburg, Würzburg 97074, Germany
- ⁵⁹ Yale University, New Haven, CT 06520

Work supported in part by the US Department of Energy under contracts DE-AC02-76CH03000, DE-AC02-98CH10886, DE-AC03-76SF00098, DE-AC03-76SF00515, and W-7405-ENG-048, and by the National Science Foundation under contract PHY-9809799.

CONTENTS

1. Introduction.....	1
----------------------	---

Linear Collider Physics Report

2. “The Case for a 500 GeV e^+e^- Linear Collider”	7
1 Introduction	7
2 Lepton colliders and the long-term future of high energy physics.....	10
2.1 A 20-year goal for high energy physics	10
2.2 A 20-year program for accelerators.....	12
3 Parameters of a 500 GeV linear collider	14
4 Why we expect new physics below 500 GeV	16
4.1 A fundamental versus composite Higgs boson	17
4.2 A fundamental Higgs boson should be light	20
4.3 The constraint on the Higgs mass from precision electroweak data.....	21
4.4 The lightest supersymmetry partners are likely to appear at 500 GeV ...	22
4.5 What if there is no fundamental Higgs boson?	24
4.6 What if the LHC sees no new physics?	26
5 Physics at a 500 GeV linear collider	27
5.1 Study of the Higgs boson	29
5.1.1 Discovery of the Higgs independent of its decay modes	30
5.1.2 Measurement of the Higgs branching ratios.....	33
5.1.3 Measurement of the Higgs boson width	35
5.1.4 Measurement of the spin-parity and CP of the Higgs boson	36
5.1.5 Measurement of the Higgs self couplings	37
5.2 Studies of supersymmetry	37
5.2.1 Slepton mass measurement.....	39
5.2.2 Slepton properties	41
5.2.3 Chargino mass measurement.....	44
5.2.4 Analysis of chargino mixing.....	45
5.3 Studies of the top quark	47
5.4 Studies of W boson couplings.....	49
5.5 Studies of QCD.....	51
5.6 Precision electroweak studies.....	52
6 Further topics from the linear collider physics program	53
6.1 Extended Higgs sector	54
6.2 Supersymmetric particle studies.....	56
6.3 New Z' bosons.....	58

6.4	Large extra dimensions	59
7	Conclusions	61

Sourcebook for Linear Collider Physics

3.	Higgs Bosons at the Linear Collider	73
1	Introduction	73
2	Expectations for electroweak symmetry breaking	75
3	The Standard Model Higgs boson—theory	79
3.1	Standard Model Higgs boson decay modes	79
3.2	Standard Model Higgs boson production at the LC	80
4	SM Higgs searches before the linear collider	83
4.1	Direct search limits from LEP	83
4.2	Implications of precision electroweak measurements	83
4.3	Expectations for Tevatron searches	84
4.4	Expectations for LHC searches	86
5	Higgs bosons in low-energy supersymmetry	88
5.1	MSSM Higgs sector at tree-level	89
5.2	The radiatively corrected MSSM Higgs sector	90
5.3	MSSM Higgs boson decay modes	95
5.4	MSSM Higgs boson production at the LC	96
6	MSSM Higgs boson searches before the LC	97
6.1	Review of direct search limits	97
6.2	MSSM Higgs searches at the Tevatron	98
6.3	MSSM Higgs searches at the LHC	99
7	Non-exotic extended Higgs sectors	102
7.1	The decoupling limit	103
7.2	Constraints from precision electroweak data and LC implications	103
7.3	Constraints on Higgs bosons with VV coupling	105
7.4	Detection of non-exotic extended Higgs sector scalars at the Tevatron and LHC	106
7.5	LC production mechanisms for non-exotic extended Higgs sector scalars	107
8	Measurements of Higgs boson properties at the LC	109
8.1	Mass	109
8.2	Coupling determinations—light Higgs bosons	112
8.2.1	Cross sections	112
8.2.2	Branching ratios	113
8.2.3	Radiative production and $t\bar{t}h$ coupling	115
8.2.4	Higgs self-coupling	115

8.2.5	Implications for the MSSM Higgs sector	115
8.3	Coupling determinations—intermediate mass Higgs bosons	117
8.3.1	Cross sections	118
8.3.2	Branching ratios	118
8.4	Coupling determinations—heavy Higgs bosons	119
8.4.1	Cross sections	119
8.4.2	Branching ratios	119
8.5	Summary of couplings	120
8.6	Total width	121
8.7	Quantum numbers	121
8.8	Precision studies of non-SM-like Higgs bosons	124
9	The Giga-Z option—implications for the Higgs sector	124
9.1	The MSSM context	125
9.2	Non-exotic extended Higgs sector context	126
10	The $\gamma\gamma$ collider option	127
11	Exotic Higgs sectors and other possibilities	130
11.1	A triplet Higgs sector	130
11.2	Pseudo Nambu Goldstone bosons	131
4.	Supersymmetry Studies at the Linear Collider	141
1	Introduction	141
2	The scale of supersymmetry	142
2.1	Naturalness	142
2.2	Neutralino relic abundance	145
2.3	Higgs mass and precision electroweak constraints	146
2.4	Evidence for new physics	146
3	Determination of masses and couplings	148
3.1	Measurement of superpartner masses	148
3.2	Measurement of supersymmetry parameters	153
4	Tests of supersymmetry	155
4.1	Confirming supersymmetry	156
4.2	Super-oblique corrections	156
4.3	Measurements at linear colliders	157
5	Symmetry violating phenomena	159
5.1	R-parity violation	159
5.1.1	$\lambda_{LLe^c} \neq 0$	160
5.1.2	$\lambda'_{LQd^c} \neq 0$	161
5.1.3	$\lambda''_{u^c d^c d^c} \neq 0$	161
5.1.4	$\mu_i \neq 0$	162
5.2	Lepton flavor violation	162

5.3	CP violation.....	163
6	Supersymmetry and e^-e^- , $e^-\gamma$, and $\gamma\gamma$ colliders.....	166
6.1	Supersymmetry and e^-e^- colliders.....	166
6.1.1	Masses.....	166
6.1.2	Mixings.....	167
6.1.3	Couplings.....	168
6.2	Supersymmetry and $e^-\gamma$ colliders.....	168
6.3	Supersymmetry at $\gamma\gamma$ colliders.....	168
7	Comparison with LHC.....	169
5.	New Physics at the TeV Scale and Beyond.....	185
1	Introduction.....	185
2	Gauge boson self-couplings.....	187
2.1	Triple gauge boson coupling overview.....	187
2.2	Triple gauge boson measurements.....	188
2.3	Electroweak radiative corrections to $e^+e^- \rightarrow 4$ fermions.....	191
2.4	Quartic gauge boson couplings.....	193
3	Strongly coupled theories.....	195
3.1	Strong WW scattering and technicolor.....	195
3.2	Composite Higgs models.....	198
4	Contact interactions and compositeness.....	201
5	New particles in extended gauge sectors and GUTs.....	202
5.1	Extended gauge sectors.....	202
5.1.1	Z' discovery limits and identification.....	203
5.1.2	W' discovery limits and identification.....	204
5.2	Leptoquarks.....	208
5.3	Exotic fermions.....	209
6	Extra dimensions.....	210
6.1	Large extra dimensions.....	212
6.2	Localized gravity.....	218
6.3	TeV-scale extra dimensions.....	222
7	Highly non-conventional theories and possible surprises.....	225
7.1	String resonances.....	225
7.2	Non-commutative field theories.....	226
8	Determining the origin of new physics.....	228
9	Conclusions.....	230
6.	Top Quark Physics.....	239
1	Introduction.....	239
2	Physics in the threshold region.....	239

2.1	Introduction	239
2.2	QCD dynamics and cross section	239
2.3	Top width	241
2.4	Top quark Yukawa coupling	241
2.5	Experimental issues	242
3	Physics above the top threshold	242
3.1	Determination of the top quark–Higgs Yukawa coupling	242
3.1.1	Introduction	242
3.1.2	Basic scenario	243
3.1.3	Analysis	243
3.1.4	Conclusion	245
3.2	Top mass reconstruction	245
3.3	Anomalous couplings	247
3.4	QCD and electroweak radiative corrections	248
4	Conclusions	251
7.	QCD and Two-Photon Physics	255
1	Introduction	255
2	QCD from annihilation processes	255
2.1	The precise determination of α_s	255
2.1.1	Event observables in e^+e^- annihilation	256
2.1.2	The $t\bar{t}(g)$ system	257
2.1.3	A high-luminosity run at the Z^0 resonance	257
2.2	Q^2 evolution of α_s	257
2.3	Top quark strong moments	259
3	Two-photon physics	260
3.1	Experimental requirements	261
3.2	Bremsstrahlung photon beam	261
3.2.1	Backscattered laser beam	262
3.3	Photon structure	262
3.3.1	$\gamma^*\gamma$ scattering— $e\gamma$ DIS	263
3.4	$\gamma\gamma$ scattering—total cross section	264
3.5	$\gamma^*\gamma^*$ scattering—QCD dynamics	265
3.6	Summary of two-photon physics	268
4	Overall summary and conclusions	268
8.	Precision Studies at the Z and the WW Threshold	271
1	Electroweak observables on the Z resonance	271
1.1	Machine issues	272
1.2	Electroweak observables	273

1.2.1	Observables from the Z resonance line scan	273
1.2.2	The effective weak mixing angle	274
1.2.3	Observables with tagged quarks	276
2	m_W from WW threshold running	277
2.1	m_W from a polarized threshold scan	278
2.2	Conclusion	279
3	Electroweak tests of the Standard Model	279
3.1	Parameterizations of deviations from the Standard Model	282
3.2	Tests of supersymmetry	284
4	Heavy flavor physics	286
4.1	Measurement prospects for $\mathcal{B}(B \rightarrow \pi^0 \pi^0)$	287
4.2	$B \rightarrow X_q \nu \bar{\nu}$	288
4.3	Semileptonic B_s decays	288
4.4	Weak decays of polarized beauty baryons	289
5	Summary	291

Pathways Beyond the Standard Model

9.	Pathways Beyond the Standard Model	299
1	Introduction	299
2	Beyond the Standard Model	300
3	Supersymmetry	301
4	New strong interactions at the TeV scale	305
4.1	Composite Higgs models	306
4.2	Technicolor theories	307
5	Extra spatial dimensions	309
5.1	Flat extra dimensions, containing only gravity	310
5.2	Warped extra dimensions, containing only gravity	311
5.3	Flat extra dimensions, containing SM gauge fields	311
5.4	Flat extra dimensions, containing all SM particles	311
6	Surprises	312

Experimental Program Issues

10.	Scenarios for Linear Collider Running	315
1	Preliminaries	315
2	Illustrative scenarios	317
2.1	A Higgs boson, but no other new physics, is seen at the LHC	317
2.2	No Higgs boson or other new particles are seen at the LHC	318
2.3	Light Higgs and superpartners are seen at the LHC	318

11. Interaction Regions	321
1 Introduction	321
2 The two interaction region design at TESLA	322
3 The dual-energy interaction region design at the NLC	322
3.1 The low-energy interaction region at the NLC	326
3.2 The high-energy interaction region at the NLC	329
3.3 Alternative interaction region scenarios	330
3.4 Simultaneous operation	332
12. Positron Polarization	333
1 Introduction	333
2 The physics perspective	334
2.1 The structure of electroweak interactions at high energies	334
2.2 Standard Model-like Higgs boson	336
2.3 Supersymmetric particle production	337
2.3.1 Slepton and squark production	337
2.3.2 Chargino and neutralino production	338
2.4 Some other new physics	339
2.5 Transverse polarization	339
3 Experimental issues	340
3.1 Polarimetry	340
3.2 Frequency of spin flips	341
3.3 Run time strategy for LL, LR, RL, RR	341
4 Sources of polarized positrons	341
4.1 Helical undulator	342
4.2 Backscattered laser	343
5 Conclusions	343
13. Photon Collider	347
1 Introduction	347
2 Physics Studies at a $\gamma\gamma$ Collider	348
2.1 Production of Higgs bosons	348
2.2 Supersymmetric particle production	349
2.3 $\gamma\gamma \rightarrow W^+W^-$ and $\gamma e \rightarrow W\nu$	350
2.4 $\gamma\gamma \rightarrow t\bar{t}$	351
2.5 Other processes	352
3 Compton Backscattering for $\gamma\gamma$ Collisions	352
3.1 Introduction	352
3.2 Photon spectra	352

3.2.1	Accelerator modifications	355
3.3	Interaction region design and backgrounds	357
4	IR optical system	357
4.1	Optics design	357
4.2	Beam pipe modifications	358
5	Laser system	359
5.1	Requirements and overview	359
5.2	Laser system front end	359
5.3	Mercury amplifier	361
5.4	Multiplexer and beam transport	363
5.5	Compressor / stretcher	363
5.6	Laser facility, systems design and risk reduction	364
14.	e^-e^- Collisions	369
1	General characteristics of e^-e^- collisions	369
2	Physics at e^-e^- colliders	370
2.1	Møller scattering	370
2.2	Higgs bosons	370
2.3	Supersymmetry	371
2.4	Bileptons	371
2.5	Other physics	372
3	Accelerator and experimental issues	373
3.1	Machine design	373
3.2	Interaction region	374
3.3	Detectors	375
4	Conclusions	375

Detectors for the Linear Collider

15.	Detectors for the Linear Collider	379
1	Introduction	379
2	Interaction region issues for the detector	379
2.1	Time structure	379
2.2	IR layout	380
2.3	Small spot size issues	382
2.4	The beam-beam interaction	382
3	Subsystem considerations	385
3.1	Vertex detector	385
3.2	Tracking	387
3.3	Calorimetry	388

3.3.1	Energy flow	388
3.3.2	Resolution, segmentation, and other requirements	389
3.3.3	Technology options	391
3.4	Muon detection	392
3.5	Solenoid	394
3.6	Particle ID	394
3.7	Electronics and data acquisition	395
4	Detectors	397
4.1	L detector for the high-energy IR	397
4.2	SD detector for the high energy IR	404
4.3	P detector for the lower-energy IR	409
4.4	Cost estimates	412

16. Questions for Further Study

	Suggested Study Questions on LC Physics and Experimentation	417
1	Physics issues	417
1.1	Higgs physics	417
1.2	Supersymmetry	418
1.3	New physics at the TeV scale	419
1.4	Top quark physics	419
1.5	QCD and two-photon physics	420
1.6	Precision electroweak measurements	420
2	Accelerator issues	421
2.1	Running scenarios	421
2.2	Machine configuration	421
2.3	Positron polarization	422
2.4	Photon collider	422
2.5	e^-e^-	423
2.6	Fixed Target	423
3	Detector issues	423
3.1	Detectors	423

Chapter 1 Introduction

The American particle physics community can look forward to a well- conceived and vital program of experimentation for the next ten years, using both colliders and fixed target beams to study a wide variety of pressing questions. Beyond 2010, these programs will be reaching the end of their expected lives. The CERN LHC will provide an experimental program of the first importance. But beyond the LHC, the American community needs a coherent plan. The Snowmass 2001 Workshop and the deliberations of the HEPAP subpanel offer a rare opportunity to engage the full community in planning our future for the next decade or more.

A major accelerator project requires a decade from the beginning of an engineering design to the receipt of the first data. So it is now time to decide whether to begin a new accelerator project that will operate in the years soon after 2010. We believe that the world high-energy physics community needs such a project. With the great promise of discovery in physics at the next energy scale, and with the opportunity for the uncovering of profound insights, we cannot allow our field to contract to a single experimental program at a single laboratory in the world.

We believe that an e^+e^- linear collider is an excellent choice for the next major project in high-energy physics. Applying experimental techniques very different from those used at hadron colliders, an e^+e^- linear collider will allow us to build on the discoveries made at the Tevatron and the LHC, and to add a level of precision and clarity that will be necessary to understand the physics of the next energy scale. It is not necessary to anticipate specific results from the hadron collider programs to argue for constructing an e^+e^- linear collider; in any scenario that is now discussed, physics will benefit from the new information that e^+e^- experiments can provide.

This last point merits further emphasis. If a new accelerator could be designed and built in a few years, it would make sense to wait for the results of each accelerator before planning the next one. Thus, we would wait for the results from the Tevatron before planning the LHC experiments, and wait for the LHC before planning any later stage. In reality accelerators require a long time to construct, and they require such specialized resources and human talent that delay can cripple what would be promising opportunities. In any event, we believe that the case for the linear collider is so compelling and robust that we can justify this facility on the basis of our current knowledge, even before the Tevatron and LHC experiments are done.

The physics prospects for the linear collider have been studied intensively for more than a decade, and arguments for the importance of its experimental program have been developed from many different points of view. This book provides an introduction and a guide to this literature. We hope that it will allow physicists

new to the consideration of linear collider physics to start from their own personal perspectives and develop their own assessments of the opportunities afforded by a linear collider.

The materials in this book are organized as follows. In Chapter 2, we reprint the ‘Linear Collider Whitepaper’, a document prepared last summer by the linear collider supporters for the Gilman writing group of HEPAP [1]. This document presents a distilled argument for the first phase of the linear collider at 500 GeV in the center of mass. Though it describes a number of physics scenarios, it emphasizes a particular perspective on the physics to be expected at the next scale. Considerable space is given to the analysis of a light Higgs boson—as called for by the precision electroweak measurements—and to measurements of supersymmetry, motivated, for example, by the precisely known values of the Standard Model coupling constants. There is no question that, in these scenarios, the linear collider would provide a program of beautiful and illuminating experiments.

The ‘Sourcebook for LC Physics’, Chapters 3–8 gives a more complete overview of the physics measurements proposed for the linear collider program. In separate sections, we review the literature that describes the measurements that the linear collider will make available on the full variety of physics topics: Higgs, supersymmetry, other models of the electroweak symmetry breaking (including new Z bosons, exotic particles, and extra dimensions), top quark physics, QCD, and the new precision electroweak physics available at linear colliders. The chapter on Higgs physics includes a thorough review of the capabilities of a linear collider for the study of the Standard Model Higgs boson as a function of its mass.

Chapter 9 gives a survey of theoretical approaches to the next scale in physics and the implications of each for the linear collider physics case. This chapter attempts to cover the full range of possibilities for physics at the next energy scale. We hope that this review will be useful in putting each particular physics scenario into a larger perspective.

The discussion of experimental program issues in Chapters 10–14 presents a number of options for the linear collider experimental program, weighing their merits and requirements. We begin by presenting some typical scenarios for operation of the linear collider, with suggested choices for energy and luminosity to meet specific physics goals. We then discuss the baseline experimental facilities. Our baseline design is an accelerator of 500 GeV center-of-mass energy, with polarized e^- beams, and with two interaction regions that share the luminosity. The design envisions a number of upgrade paths. These include low-energy precision measurements in one of the two regions and e^+e^- collisions at multi-TeV energies in the other. The logic of these plans is described in some detail. In the subsequent chapters, we discuss the possible options of positron polarization, operation of a $\gamma\gamma$ collider by laser backscattering from electron beams, and operation for e^-e^- collisions. In each case, we review the promise and the technological problems of the approach.

Chapter 15 discusses detectors for the linear collider experiments. We present and cost three detector models. We also discuss issues for the linear collider detector design. Though a generic LEP-style detector could carry out the basic measurements, the linear collider environment offers the opportunity for exceptional detection efficiencies and precision in the study of physics processes. We list a number of research problems whose solution would allow us to realize the full potential that high energy e^+e^- collisions offer.

The final chapter gives a list of suggested questions that could be taken up at Snowmass or in other studies. Many of these arise from the specific discussions of the earlier chapters. They range from questions of accelerator and detector optimizations to physics issues that require first study or more careful scrutiny.

We do not discuss linear collider accelerator designs in this book, but a number of useful reports on the various current proposals are available. TESLA, based on superconducting rf cavities, has been submitted to the German government as a formal TDR [2]. A detailed proposal for the warm cavity accelerator developed by the NLC and JLC groups was presented in the 1996 ZDR [3], and the current NLC baseline is described in a separate paper for the Snowmass 2001 workshop [4]. These two approaches have different emphases and differ in many details. However, both designs meet the requirements to achieve the physics goals that we discuss in this book.

We believe that it is urgent that the American high-energy physics community come to grips now with the issues related to the linear collider. There are several reasons for this. First, the proposals for a linear collider in Europe and in Asia are now becoming explicit. Inevitably, such proposals will raise the question of how the American community will participate. We are approaching the time when the nature of our involvement will be decided by default, not by our design. Second, the high energy frontier of accelerator-based research will pass to the LHC in only a few years. Since the health of any region's particle physics community depends on its central participation in a frontier facility, the US community needs to address how it will participate in the major facilities of the coming era. Third—and most importantly—the linear collider is very likely, in our opinion, to make major progress on the most pressing physics questions before us today. We can offer no guarantee of this, since it is the nature of our field that each new frontier accelerator steps into the unknown. But for all the ways that are foreseen to resolve the mystery of the origin of electroweak symmetry breaking, measurements at the linear collider would be of crucial importance.

References

- [1] J. Bagger *et al.* [American Linear Collider Working Group], hep-ex/0007022.
- [2] TESLA Technical Design Report, http://tesla.desy.de/new_pages/TDR_CD/start.html.
- [3] NLC Zeroth-Order Design Report, SLAC-R-474, <http://www.slac.stanford.edu/accel/nlc/zdr/>.
- [4] US NLC Collaboration, *2001 Report on the Next Linear Collider*, FERMILAB-Conf-01/075-E, LBNL-47935, SLAC-R-571.

2000 Linear Collider Physics Report

Chapter 2 “The Case for a 500 GeV e^+e^- Linear Collider”

(Report to the HEPAP Writing Group, July 2000)

Authors: J. Bagger, C. Baltay, T. Barker, T. Barklow, U. Baur, T. Bolton, J. Brau, M. Breidenbach, D. Burke, P. Burrows, L. Dixon, H. E. Fisk, R. Frey, D. Gerdes, N. Graf, P. D. Grannis, H. E. Haber, C. Hearty, S. Hertzbach, C. Heusch, J. Hewett, R. Hollebeek, R. Jacobsen, J. Jaros, T. Kamon, D. Karlen, D. Koltick, A. Kronfeld, W. Marciano, T. Markiewicz, H. Murayama, U. Nauenberg, L. Orr, F. Paige, A. Para, M. E. Peskin, F. Porter, K. Riles, M. Ronan, L. Rosenberg, B. Schumm, R. Stroynowski, S. Tkaczyk, A. S. Turcot, K. van Bibber, R. van Kooten, J. D. Wells, H. Yamamoto

Several proposals are being developed around the world for an e^+e^- linear collider with an initial center of mass energy of 500 GeV. In this paper, we will discuss why a project of this type deserves priority as the next major initiative in high energy physics.

1 Introduction

Those of us who have chosen to work in elementary particle physics have taken on the task of uncovering the laws of Nature at the smallest distance scales. The process is an excavation, and as such, the work proceeds through various stages. During the past ten years, experiments have clarified the basic structure of the strong, weak, and electromagnetic interactions through measurements of exquisite precision. Now the next stage is about to begin.

The structure of the electroweak interactions, confirmed in great detail by recent experiments, requires a new threshold in fundamental physics at distances or energies within a factor of ten beyond those we can currently probe. More detailed aspects of the data argue that this threshold is close at hand. In the next decade, we will carry out the first experiments that move beyond this threshold, perhaps at the Fermilab Tevatron, almost certainly at the CERN LHC.

Many measurements of this new physics will be made at these hadron colliders. In this document we will argue that electron-positron colliders also have an important role to play. Because the electron is an essentially structureless particle which interacts through the precisely calculable weak and electromagnetic interactions, an e^+e^-

collider can unambiguously determine the spins and quantum numbers of new particles. Cross section and branching ratio measurements are straightforward and can be readily compared to models for the underlying physics. Electron beam polarization allows experiments to distinguish electroweak quantum numbers and measure important mixing angles. During the next few years, hadron colliders will likely discover the agents of electroweak symmetry breaking. But electron-positron experiments will also be necessary to completely determine the properties of the new particles.

We believe that a number of new developments call for the start of construction of a high luminosity 500 GeV e^+e^- collider in this decade. First, precision measurements from experiments at CERN, Fermilab and SLAC suggest that important new physics is within range of this machine. Second, the necessary technologies have been developed to the point where it is feasible to construct the collider. Third, these technologies, and others still under development, should allow the collider to be upgraded to TeV and even multi-TeV energies. For all of these reasons, we believe that the time is right to design and construct a high luminosity 500 GeV e^+e^- linear collider.

In this paper, we formulate the physics case for this machine. The elements of the argument are:

1. New physics processes should appear at a 500 GeV collider. In particular, precision data indicate that the Higgs boson should be accessible to this machine. If it is, the collider will definitively test whether the Higgs boson is responsible for generating the masses of the quarks, leptons, and gauge bosons of the Standard Model.
2. There are good reasons to believe that there is other new physics at the TeV scale. Across the range of models, e^+e^- collider experiments add crucial information to that available from hadron collider experiments. They will dramatically clarify our understanding of TeV scale physics.
3. A 500 GeV collider is a critical first step toward a higher energy e^+e^- collider. We believe that such a machine is likely to be needed for the complete elucidation of the next set of physical laws.

This paper will proceed as follows: In Section 2, we will discuss the future of high energy physics from a long-term perspective. We will briefly review the recent developments that have clarified the structure of elementary particle interactions, the challenges posed by the next scale in physics, and the need for higher energy lepton and hadron colliders. In Section 3, we will briefly describe the current designs of 500 GeV e^+e^- colliders and the technologies that will enable them to be upgraded to higher energy. This discussion will define the basic accelerator specifications that we will explore in this study: center of mass energies up to 500 GeV, and luminosity samples of 200 fb^{-1} to 600 fb^{-1} . In Section 4, we will give the arguments that

new physics should appear at 500 GeV. In Section 5, we will describe some of the important measurements that could be made at a 500 GeV collider, or with high luminosity measurements at the Z pole or the WW threshold. In Section 6, we will describe additional measurements for which the required energy is less certain but which, when they are kinematically accessible in e^+e^- collisions, will beautifully enhance the results of the LHC. Section 7 contains our conclusions.

There is an enormous literature on the physics capabilities of e^+e^- colliders at energies of 500 GeV and above. Our goal in this document is to summarize and focus this information. Much more information about the capabilities of a high energy e^+e^- linear collider can be found in [1,2,3,4] and references therein.

Before beginning our discussion, we would like to comment on three related issues. The first is the role of the LHC. The ATLAS and CMS experiments at the LHC are likely to be the most important high energy physics experiments of the decade, precisely because they will be the first experiments whose energy is clearly in the regime of new physics. The linear collider does not need to compete directly with the LHC in terms of energy; instead, its physics program should complement the LHC by adding important new information. It is just for this reason that we must look at the strengths and weaknesses of the LHC when we build the case for an e^+e^- linear collider.

The second concerns the competing linear collider technologies, the approach of NLC and JLC, with warm copper accelerating structures, and that of TESLA, with superconducting RF cavities. From the point of view of the physics, the similarities of these proposals are more important than their differences. Both schemes are capable of high luminosity ($2 \times 10^{34} \text{ cm}^{-2}\text{sec}^{-1}$ for NLC/JLC, $3 \times 10^{34} \text{ cm}^{-2}\text{sec}^{-1}$ for TESLA) and lead to similar backgrounds from beamstrahlung, pair production, and other machine-related effects. The physics case we will develop applies to both schemes. A decision between them must eventually be made on the basis of cost, detailed technical advantages, and upgradability, but we will not argue for either particular approach in this report.

The third issue concerns the ultimate upgrade of the energy of the e^+e^- collider to multi-TeV center of mass energies. Recent R&D suggests that this may be achievable. It is likely that the needs of physics will eventually call for experiments at such high energies, and so the collider should be planned to support a program of successive energy upgrades. However, the first stage of any program toward multi-TeV e^+e^- collisions will be a 500 GeV linear collider. This first-stage machine now has a clear physics justification, and that will be the main focus of this report.

2 Lepton colliders and the long-term future of high energy physics

The accelerators at CERN, Fermilab, DESY, and SLAC, which today provide the highest energy particle collisions, were originally envisioned and justified in an era when the fundamental structures of the strong and weak interactions were completely mysterious. These facilities provided much of the data that allowed these mysteries to be understood. Through successive upgrades and improvements, they also provided the data that allowed the resulting theories to be tested with precision. We have learned that with time, accelerators and individual experiments outstrip predictions of their physics reach. This history implies that we should think about future accelerators from a long-term perspective. We begin this report with that discussion. Where may we expect to be, 20 years from now, in our exploration of fundamental physics? How can we get there?

2.1 A 20-year goal for high energy physics

The beautiful experiments in particle physics over the past 20 years have brought us to the point where we are poised to discover the microphysical origin of mass. In the Standard Model, the electroweak interactions are built on the foundation of an $SU(2) \times U(1)$ gauge symmetry. All of the mass terms in the Standard Model necessarily violate this symmetry. Masses can only appear because some new fields cause this symmetry to be spontaneously broken.

The spontaneous symmetry breaking cannot be explained in terms of the known strong, weak, and electromagnetic interactions. In the 1980s, it was possible to believe that the W and Z bosons were composite particles [5,6,7,8]. In the 1990s, when electroweak radiative corrections were measured to be in agreement with the $SU(2) \times U(1)$ gauge theory [9], this possibility was swept away. At the same time, the fundamental couplings of the strong, weak, and electromagnetic interactions were precisely measured. At the weak interaction scale, these couplings are too small to create a new state of spontaneously broken symmetry. Thus, the breaking of the electroweak gauge symmetry must come from new fundamental interactions. To explain the magnitude of the W and Z masses, these interactions must operate at the TeV scale.

Over the next 20 years, a primary goal for high energy physics will be to discover these new fundamental interactions, to learn their qualitative character, and to describe them quantitatively by new physical laws. Today, although we can guess, we do not know what form these laws will take. It is logically possible that the electroweak symmetry is broken by a single Higgs boson. More likely, the agent of symmetry breaking will be accompanied by other new physics. A popular hypothesis is a supersymmetric generalization of the Standard Model. Other suggestions include models

with new gauge interactions, leading to a strongly-coupled theory at TeV energies, and models with extra spatial dimensions and quantum gravity at the TeV scale.

Aside from their own intrinsic importance, the study of these new interactions will play a crucial role in our understanding of the universe. For example, supersymmetry is a theory of space-time structure which requires modification of the theory of gravity. Other types of models, in particular those with large extra space dimensions, necessarily invoke new space-time physics at the TeV scale.

New physics is also needed to address one of the mysteries of cosmology. There is substantial evidence that a large fraction of the total energy density of the universe is composed of non-baryonic dark matter. Recent estimates require that dark matter should make up more than 80% of the total matter in the universe [10]. A new stable particle with a mass of about 100 GeV and an annihilation cross section of electroweak size is an excellent candidate for this dark matter. Models of electroweak symmetry breaking typically contain a particle filling this description. During recent years, an enormous amount has been learned about the early universe, back to a time of about 1 second after the Big Bang, by the detailed comparison of primordial element abundances with a kinetic theory of nucleosynthesis based on measured nuclear physics cross sections [11]. In 20 years, we could have a precise knowledge of these new interactions that would allow a predictive kinetic theory of the dark matter. This would push our detailed knowledge of the early universe back to 10^{-12} seconds after the Big Bang.

High energy physics has many concerns aside from the nature of electroweak symmetry breaking. The origin of the quark and lepton flavors is mysterious; the pattern of masses and flavor mixings is not understood. The discovery that neutrinos have mass [12] has added a new dimension to this puzzle. In this decade, there will be a significant effort, with contributions from many laboratories, to measure the parameters of flavor mixing and CP violation. These questions are all intimately related to the puzzle of electroweak symmetry breaking.

There are two reasons for this. First, in the Standard Model all mass terms are forbidden by symmetry, and therefore all masses, mixings, and CP violating terms must involve the symmetry-breaking fields. For example, in a model in which this breaking is due to fundamental Higgs bosons, the quark and lepton masses, mixings, and CP violating angles originate in the fermion couplings to the Higgs fields. We will need to know what Higgs bosons exist, or what replaces them, in order to build a theory of flavor. Second, deviations from the conventional expectations for flavor physics are necessarily due to new particles from outside the Standard Model. If such deviations are to be visible in the study of CP violation, for example, the new particles must typically have masses of one to several hundred GeV. Given this mass scale, it is likely that those particles are associated with the physics of electroweak symmetry breaking.

Precision low energy experiments are designed to search for deviations from the

Standard Model. Such deviations indicate the presence of new particles which must be found at high energies. Models of new physics do not always predict such deviations, and observed effects can be interpreted in multiple ways. So, there is no way to escape the need to search for new particles directly at high energy. In fact, we are *already* in a situation where our current knowledge requires that new physics be found at the next step in energy. The need for new accelerators can be seen from our study of the weak interactions, as a consequence of the laws that we have established experimentally in the past decade.

Thus, the elucidation of electroweak symmetry breaking should be the key central goal for particle physics research in the next 20 years.

2.2 A 20-year program for accelerators

As we have just seen, electroweak symmetry breaking requires new fundamental interactions; it is our task to find and understand them. In every example we know of a fundamental law of Nature (with the possible exception of Einstein's general relativity), the correct theoretical understanding arose only with the accumulation of a large stock of experimental data and the resolution of paradoxes within that data. New and varied experimental techniques were needed, both to accumulate the basic data, and to crucially check or refute intermediate hypotheses.

For the direct exploration of the TeV energy scale, only two types of collision processes are feasible—proton-proton and lepton-lepton reactions. Proton-proton collisions have the advantage of very high center of mass energies and high rates. However, this environment also has large backgrounds, mainly from Standard Model gluon-gluon collisions. Uncertainties from parton distributions and from perturbative calculations limit the accuracy possible in many precision measurements. Lepton-lepton collisions have a complementary set of advantages and disadvantages. The cross sections are low, requiring high luminosity. However, new physics processes, if they occur, typically form a large fraction of the total cross section. Final states can be observed above well understood backgrounds, allowing unambiguous theoretical interpretation. Cross sections for signal and background processes can be computed to part-per-mil accuracy. Lepton-lepton collisions provide precise and model-independent measurements which complement those from hadron machines.

It is well appreciated that, in developing our understanding of the strong and electroweak interactions, proton and electron colliders made distinct and complementary contributions. As representative examples, recall the discovery of nucleon and meson resonances, the Υ , and the Z^0 and W^\pm at proton facilities and the corresponding studies of deep inelastic scattering, the charmonium and bottomonium systems, the Z^0 resonance, and the W^+W^- threshold at electron machines. In a natural evolution, results from e^+e^- have pointed to new processes in D and B meson decays which have been probed further in high-rate hadron experiments. In the later sections of

this report, we will discuss a number of specific models that illustrate the way this complementarity might play out at higher energies.

This logic leads us to plan, over the next 20 years, to study the new interactions responsible for electroweak symmetry breaking in both proton-proton and lepton-lepton collisions. From our experience with the strong and electroweak interactions, it is likely that these new interactions will not be thoroughly understood until we can look at them experimentally from energies above the relevant particle masses. In some supersymmetric models, it is possible to stand above the whole spectrum at a center of mass energy of 1 TeV. But quite possibly—and necessarily for models of strong-interaction electroweak symmetry breaking—this requires much higher energies, perhaps 5–10 TeV in parton-parton collisions.

This challenge was the motivation for building the SSC. With the anticipated start of the LHC experimental program in 2005, the proton-proton program will at last begin. The LHC, operating at 14 TeV and a luminosity of 10^{34} cm⁻²sec⁻¹, has parton collisions of sufficiently high energy that it is expected to produce some signature of the new physics that underlies electroweak symmetry breaking [13,14,15].

For electron-positron colliders, all schemes for achieving high energy collisions involve linear colliders. The technology of e^+e^- linear colliders is relatively new, but important expertise was gained through operation of the SLC [16], which operated at the Z^0 pole. The natural next step for this technology is a collider with 500 GeV center of mass energy. A collider providing this energy, and delivering the required luminosity, above 10^{34} cm⁻²sec⁻¹, would be a critical step on the path toward multi-TeV energies and very high luminosities. At the same time, as we shall see, a 500 GeV collider has sufficient energy to make decisive contributions to the study of electroweak symmetry breaking.

The design of a 500 GeV linear collider must not preclude extension to higher energies. Indeed, both the current warm and superconducting linear collider proposals explicitly include adiabatic extensions to somewhat higher energies. TESLA allows a stage of operation at 800 GeV. The NLC/JLC plan includes ready expansion to 1 TeV and allows for an upgrade to 1.5 TeV. The pace of such an upgrade would depend on the physics found at the LHC, as well as on results from the first phase of 500 GeV operation.

In the context of a 20-year plan, however, we must go even further, and contemplate partonic collision energies of 5–10 TeV. For hadron colliders, the VLHC program of R&D now underway, or potential upgrades to the LHC, could provide this; however it seems premature to propose such a machine until the initial LHC results are available. A multi-TeV muon collider has received much recent attention, but there remain important R&D issues to be resolved before its feasibility can be determined. In the past few years, a promising route to multi-TeV collisions has emerged for e^+e^- colliders. The possibility of a 5 TeV e^+e^- linear collider was studied at Snowmass '96 [17], where three outstanding problems were identified: the lack of a feasible RF power

source for high frequency accelerating structures, the large length of the Final Focus sections, and the tight manufacturing and alignment tolerances for the accelerating structures. Since then, there has been considerable progress. A major rethinking of the two-beam (CLIC) acceleration scheme makes this concept, in which a low-energy, high-current beam is used to generate high-frequency RF, look promising as a power source for very high energy acceleration [18]. Indeed, such schemes now look feasible for lower RF frequencies (for example, at X band), and this could provide a natural evolution path to higher accelerating gradients [19]. New compact Final Focus layouts [20] have been recently incorporated into the NLC design.

The issue of manufacturing and alignment tolerances is central to the successful operation of any high-luminosity linear collider. This issue is presented in a more manageable form in the design of a 500 GeV collider with either warm or superconducting RF. Moreover, the experience of building and running this machine will be an invaluable prerequisite to eventual e^+e^- experimentation at multi-TeV energies. In addition, any multi-TeV e^+e^- linear collider will be placed in a long, straight tunnel exactly like the one on the site of a 500 GeV machine and perhaps could reuse the damping rings and injector complex of the 500 GeV stage. Thus, a 500 GeV linear collider is the first stage of a 20-year exploration in e^+e^- physics.

3 Parameters of a 500 GeV linear collider

The designs of linear colliders have evolved dramatically over the past five years, based in part on experience from the SLAC Linear Collider operating at 91 GeV, and in part on extensive collaborative R&D efforts in Europe, Japan and the United States. At this writing, the machine parameters are still being evaluated; this section is intended to give the currently envisioned scope of the possible accelerator projects.

The TESLA collider, developed by a collaboration led by DESY, would employ superconducting RF accelerating cavities operating in L-band (1.3 GHz). The JLC (KEK) and NLC (SLAC, LBNL, LLNL, FNAL) designs are based on warm accelerating structures operating in X-band (11.4 GHz). Initial construction of each of these is expected for a 500 GeV machine. A variety of important differences in the designs follow from the basic choice of accelerating frequency. (KEK is also considering a C-band variant operating at 5.7 GHz.)

The main parameters of TESLA and the X-band NLC/JLC are shown in Table 1. For all proposals, electron beam polarization of 80% is expected. Production of polarized positrons can be envisioned by creating polarized photons in sophisticated undulator magnets, or by backscattering polarized high-power lasers, but these possibilities require further development. In all proposals, the collider can also be operated for e^-e^- collisions with some loss in luminosity. By backscattering laser beams, it may be possible to create a high-luminosity gamma-gamma collider with a center of

	TESLA	NLC/JLC
E_{CM} (GeV)	500	500
RF frequency (GHz)	1.3	11.4
Repetition rate (Hz)	5	120
Luminosity ($10^{34} \text{ cm}^{-2}\text{sec}^{-1}$)	3.4	2.2
Bunch separation (ns)	337	1.4
Effective gradient (MV/m)	22	50.2
Beamstrahlung (%)	3.3	4.6
Linac length (km)	31	10.8

Table 2.1: Basic parameters of the high-luminosity TESLA and NLC/JLC accelerator designs.

mass energy of about 80% of that for e^+e^- .

The U.S. design of the NLC underwent a DOE readiness review to initiate the Conceptual Design Report in May 1999. The Review Committee was positive in its assessment of the technical design. The cost was estimated at \$7.9B. After subtraction of contingency, escalation, and detectors, these costs were distributed over the major subsystems as follows: injectors (19%), main linacs (39%), beam delivery (11%), global costs (17%), management/business (14%). The DOE decided not to proceed with the official CD-1 milestone in view of this cost. Present work is focused on cost and possible scope reductions. In the past year, progress has been made in identifying areas of savings, including the use of permanent magnets for the beam lines, electronics distributed along the linacs, modifications to the injectors, and considerable reduction of the length of the Final Focus. Demonstrated improvements in the klystrons and modulators should give a reduction of RF power costs. Taken together, these developments are estimated to reduce the cost by 30%. Scope reductions, including building the linacs initially for 500 GeV operation, with subsequent civil construction for higher energy, could yield a further 10–15% reduction in the initial cost.

The luminosity expected for the NLC design depends critically on the precision with which one can build and align the disk-loaded accelerating structures of the main X-band linac. Recent tests have demonstrated that structures can be produced with 2–3 times better accuracy than projected in the 1999 review, and that monitors built into these structures can measure their position with respect to the beam to within a few microns. Re-examination of the beam parameters in the light of these results has led to the realization that the luminosity of the collider can be expected to be 3–4 times higher than projected in 1999, although it is likely to require some period of running to carry out the needed beam-based alignment of the accelerator. It is reasonable to assume that the collider will begin operation at $5 \times 10^{33} \text{ cm}^{-2}\text{sec}^{-1}$ and

that, over a period of time, it will reach the design luminosity of $2.2 \times 10^{34} \text{cm}^{-2} \text{sec}^{-1}$ shown in Table 1. This would yield 100fb^{-1} of accumulated data in the first year of operation and $200 \text{fb}^{-1}/\text{yr}$ in subsequent years.

Each of these proposals includes possible adiabatic upgrades in energy. The TESLA collider can be expanded to 800 GeV through higher accelerating gradients. The NLC/JLC energy upgrade to 1 TeV could be achieved through an increase in the linac lengths and the addition of more RF structures. Improvements in RF gradients or further increases in length could allow operation at 1.5 TeV. It is important for the long term evolution of the linear collider that the flexibility to implement these options be included in the initial machine design.

Work has been done at CERN (CLIC) to develop the RF power for acceleration to even higher energies. The idea is to generate wakefield power for the main linacs using a high current, low energy drive beam operating at low (L-band) frequencies. Recent work at SLAC has expanded this concept to incorporate a recycling drive beam train that is cheaper, more compact and efficient than the original CLIC concept. Accelerating gradients of about 100 MV/m are envisioned for this two beam design. The two beam linear collider offers an attractive possibility for later expansion of the linear collider to multi-TeV operation, and suggests the potential for an evolving accelerator facility that can follow the initial phase of physics results. Recent R&D suggests that the use of the two beam drive technology is as well suited for linacs operating in the X-band as for the 30 GHz structures originally envisioned by CLIC, although the limits to feasible gradients are not clear.

For the NLC design with permanent magnets in the beam lines, the energy for operation cannot be decreased below half its maximum. As discussed in the next sections, physics considerations may dictate that a wider range of energies is needed. In particular, a return to the Z^0 pole may be desirable to improve the precision of the electroweak measurements. Similarly, if the Higgs boson is in the low mass region favored by the Standard Model or supersymmetry, it may be advantageous to accumulate substantial integrated luminosity at the energy of the maximum Higgs cross section and, at the same time, explore the high energy region. Recently, consideration has been given to providing a second beam operating at lower energies. This beam would be extracted from the main accelerator and accelerated in unused time slices of the AC duty cycle. The extra power needed for this operation could be low because of the reduced energy of the beams. Low and high energy beams would be delivered to dedicated detectors installed at separate interaction points in the beam delivery region.

4 Why we expect new physics below 500 GeV

At Snowmass '96, it was argued that a 1.5 TeV e^+e^- collider is roughly equivalent to the LHC in its ability to detect the new physics related to electroweak symmetry breaking [15]. However, this point will certainly be moot by the time such a linear collider operates. The real question that we must address is different: *In an era in which the LHC is already exploring the new interactions responsible for electroweak symmetry breaking, what critical information must e^+e^- experiments add, and at what e^+e^- center of mass energies should this information be sought?*

Today, there is considerable evidence that an e^+e^- collider program should begin at a center of mass energy of 500 GeV. This evidence is indirect and will remain so until the new particles responsible for electroweak symmetry breaking are discovered. The case rests on the large body of precision data acquired over the past ten years. These data agree remarkably with the minimal Standard Model. When interpreted using this model, they require that the Higgs boson be light. The data also place strong constraints on possible new physics associated with electroweak symmetry breaking. These constraints define distinct pathways for new physics which will be tested at the next generation of colliders.

Following the guidance of the precision data, we will argue in this section that a 500 GeV linear collider will be needed whatever the outcome of the LHC experiments might be. In Sections 4.1–4.3, we will outline why there should be a light Higgs boson with mass below about 200 GeV. In Section 4.4, we will argue that, if the new physics includes supersymmetry, the lightest superpartners should be found at a 500 GeV collider. There are known ways to evade these arguments, but they too give rise to crucial tests in e^+e^- collisions at 500 GeV, as we will discuss in Section 4.5. Finally, in Section 4.6, we will address the question: what if the LHC sees no new physics?

4.1 A fundamental versus composite Higgs boson

Models of electroweak symmetry breaking divide into two groups at the first step. Is the symmetry breaking induced by a fundamental scalar field or by a composite object? Is electroweak symmetry breaking a weak-coupling phenomenon, or does it require new strong interactions? These basic questions have driven the study of electroweak symmetry breaking for 20 years [21,22]. Many people use analogies from QCD or superconductivity to argue against the plausibility of fundamental scalars, or use the perceived beauty of supersymmetry to motivate a fundamental scalar Higgs field. We believe that it is possible to make a preliminary judgment—in favor of a fundamental Higgs field—on the basis of the data. This will be important, because models in which the Higgs is fundamental favor a light Higgs boson, while other models favor a heavy Higgs resonance, or none at all.

The simplest model of electroweak symmetry breaking is the minimal version of the Standard Model, which introduces one elementary Higgs field and nothing else. This model is consistent with the present data, but it is totally inadequate as a physical theory. In this model, the mass parameter m^2 of the Higgs field is a free parameter which cannot be computed as a matter of principle, because it receives an infinite additive renormalization. Electroweak symmetry is broken or not according to whether this parameter, after renormalization, is positive or negative. If the infinite radiative corrections are made finite by a cutoff at some energy M , m^2 can be much less than M^2 only if the radiative corrections are finely tuned to cancel. If M is taken to be the Planck scale, these corrections must cancel in the first 30 decimal places. Theorists often consider this to be a problem in its own right (the ‘gauge hierarchy problem’). This problem is a symptom of the fact that the Standard Model is only a parametrization, and not an explanation, of electroweak symmetry breaking.

Theories of electroweak symmetry breaking can be constructed either with or without fundamental Higgs particles. The preference we have expressed for a fundamental Higgs particle is reflected in the history of the subject. Phenomenological models of supersymmetry introduced in the early 1980s [23,24,25,26] are as valid today as when they were first created. On the other hand, the predictions of the early dynamical models (as reviewed, for example, in [27]) have been found to be inconsistent with experiment, requiring major changes in model-building strategies.

To discuss this point, we must define what we mean by a ‘fundamental scalar field’. A particle which looks fundamental and structureless on one length scale can be seen to be composite on a smaller length scale. In nuclear physics, and more generally in scattering processes with energies of a few hundred MeV, the pion can be treated as a structureless particle. However, in hard QCD processes, the pion must be treated as a quark-antiquark bound state. At the other extreme, string theory predicts that even quarks and leptons have a finite size and an internal structure at the Planck scale. In almost any theory, a particle can at best be considered fundamental at some particular distance scale. The question here is whether the Higgs boson is elementary well above the scale of the new interactions responsible for electroweak symmetry breaking. In the following discussion, we use the term ‘fundamental Higgs’ for the case that there is a scalar Higgs field in the Lagrangian at an energy scale of 20 TeV.

The answer to this question has direct implications for the theory of the quark and lepton masses. These masses arise through $SU(2) \times U(1)$ symmetry breaking, from terms in the effective Lagrangian that couple left-handed to right-handed fermions. If there is a fundamental Higgs field, a typical term has the form

$$\delta\mathcal{L} = \lambda_f \bar{f}_L \phi f_R + \text{h.c.} , \tag{2.1}$$

where ϕ is an $SU(2)$ -doublet Higgs field and the coupling λ_f is dimensionless. The fermion f obtains mass when ϕ acquires a vacuum expectation value. To explain the size of the mass, a theory must contain new interactions that fix the value of λ_f .

Because λ_f is dimensionless, these interactions can occur, without prejudice, at any energy scale larger than 20 TeV. In typical models with a fundamental Higgs boson, these interactions occur at the scale of grand unification, or even above.

If there is no fundamental $SU(2)$ -doublet scalar field, the interaction (2.1) does not exist. Instead, one must write a more complicated interaction that couples $\bar{f}_L f_R$ to other new fields. For example, in technicolor models, one writes

$$\delta\mathcal{L} = \frac{g^2}{M_E^2} \bar{f}_L f_R \bar{Q}_R Q_L + \text{h.c.} , \quad (2.2)$$

where Q is a new heavy fermion with strong interactions at the TeV scale. This is a dimension-6 operator, and therefore we have written a coefficient with the dimensions (mass)⁻². If the operator $(\bar{Q}_R Q_L)$ acquires a vacuum expectation value at the TeV scale and this operator is expected to generate a 1 GeV fermion mass, M_E must be roughly 30 TeV. The four-fermion operator (2.2) can be induced by the exchange of a heavy boson of mass M_E . However, whatever the mechanism that leads to this operator, the physical interactions responsible must operate at some energy scale not too far above M_E . This means that, unlike the previous case, the interactions that determine the quark and lepton masses and mixings must occur at energies not so far above those we now probe experimentally.

In fact, these interactions must occur at sufficiently low energies that they would be expected to contribute significantly to $\mu \rightarrow e\gamma$ and $K \rightarrow \mu e$, and to $K-\bar{K}$, $B-\bar{B}$, and $D-\bar{D}$ mixing. The fact that these processes are not observed is a severe problem for dynamical theories. A further problem arises from the large size of the top quark mass. To produce a mass as large as is observed, the mass scale M_E for the top quark—and, by symmetry, for the b_L —must be close to 1 TeV. This new interaction would be expected to lead to enhanced flavor-changing neutral current amplitudes, and to few-percent corrections to the $Zb\bar{b}$ coupling [28].

These experimental observations have eliminated essentially all simple models of dynamical symmetry breaking. The only models that survive have complex new dynamics (*e.g.*, [29,30,31]) or, below energies of several TeV, behave almost exactly like the Standard Model with a scalar Higgs field (*e.g.*, [32]). Neither type of model resembles the attractive intuitive picture that first led people to explore electroweak symmetry breaking by new strong interactions.

Generalizations of the simplest Standard Model with additional fundamental scalar fields have also been proposed. But these have little motivation, and like the minimal Standard Model, the Higgs vacuum expectation value, and even the existence of electroweak symmetry breaking, cannot be predicted as a matter of principle.

The simplest models with a fundamental Higgs field in which electroweak symmetry breaking results from a calculation, rather than a parameter choice, are those with supersymmetry. Without debating the virtues or deficits of supersymmetric models, what is relevant here is that supersymmetric models have not been significantly con-

strained by the precise experimental measurements of the past 20 years. Supersymmetric particles give very small effects in electroweak precision measurements because the masses of the superparticles preserve $SU(2) \times U(1)$ gauge symmetry, and so do not require electroweak symmetry breaking. In models that decouple in this way, new particles with mass M give corrections to the Standard Model predictions at the Z^0 which are of size

$$\frac{\alpha m_Z^2}{\pi M^2} . \tag{2.3}$$

As long as we stay below the energy at which the new particles actually appear, their influence is very small. Then, as we pass the threshold, new physics appears suddenly. Supersymmetry thus naturally suppresses deviations from the Standard Model—until we begin to produce the supersymmetric particles. Models with dynamical electroweak symmetry breaking almost always contain heavy matter states which have chiral couplings and thus do not decouple from electroweak symmetry breaking. In these models, one expects significant corrections to the Standard Model well below the energy scale of the new particles.

In addition to this decoupling, the early supersymmetry models made two important predictions. The first was that the top quark mass should be heavy. This tendency arises from the fact that, in supersymmetric models, electroweak symmetry breaking can be triggered by radiative corrections due to the top quark Yukawa coupling. The papers [23,24,25,26] all quoted lower bounds on the top quark mass, ranging from 50 to 65 GeV. (Later, corners of parameter space were found in which the top quark mass could be lower.) Supersymmetry readily accommodates a top quark mass as large as 175 GeV. The second prediction was that the value of $\sin^2 \theta_w$ should be close to 0.23 (as now observed), rather than the value 0.21 preferred in the early 1980's. This prediction arises from grand unification with the renormalization group equations of supersymmetry [33,34,35]. The precise determination of α_s and the electroweak couplings at the Z^0 has given even stronger support to the idea of supersymmetric grand unification, with the issue now at the level of detailed higher-order corrections [36].

Of course it is premature to make a final decision between the different models. For this, we must discover and study the Higgs boson, or whatever takes its place. But, in planning where we should look for these phenomena, we should take into account that models with fundamental Higgs bosons passed the first tests presented by the data, while the early dynamical models did not.

4.2 A fundamental Higgs boson should be light

In the previous section, we noted that in models with fundamental Higgs bosons, the Higgs is typically light. In this section, we will quantify that statement with upper bounds on the Higgs mass.

In the Standard Model, the mass of the Higgs boson is determined in terms of the Higgs field expectation value v and the Higgs self-coupling λ by the relation

$$m_h = \sqrt{2\lambda}v, \quad (2.4)$$

with $v = 246$ GeV determined by the values of the W and Z masses. A bound on λ thus implies a bound on m_h . For example, $\lambda < 1$ implies $m_h < 350$ GeV. How large can λ reasonably be?

Like α_s , λ is a running coupling constant, but in this case radiative corrections drive λ to larger values at higher energies. Just as the running α_s diverges at $\Lambda_{\overline{MS}}$, signaling the onset of nonperturbative QCD effects, the running λ diverges at a high energy scale Λ_h . Presumably, this must signal the breakdown of the fundamental Higgs picture. The relation between Λ_h and the value of λ at the weak interaction scale can be computed from the Standard Model [37]. It is conveniently written, using (2.4), as

$$m_h = \frac{1000 \text{ GeV}}{\sqrt{\ln(\Lambda_h/v)}} \quad (2.5)$$

The value of m_h in (2.5) is the largest Higgs boson mass compatible with a Higgs field which is elementary at the scale Λ_h . For $\Lambda_h = 20$ TeV, $m_h < 500$ GeV.

A much stronger limit on m_h is obtained if one takes seriously the experimental evidence for grand unification and assumes that the Higgs boson is a fundamental particle at the grand unification (GUT) scale. If we naively put $\Lambda_h > 10^{16}$ GeV into (2.5), we find $m_h < 180$ GeV. Successful grand unification requires supersymmetry and brings in ingredients that make the computation of m_h more complex. But, detailed analysis of supersymmetric grand unified models has shown that the idea of an upper bound on m_h remains valid. In 1992, two groups presented systematic scans of the parameter space of supersymmetric grand unified theories, demonstrating the bound $m_h < 150$ GeV [38,39]. Exceptions to this constraint were later found, but still all known models satisfy $m_h < 205$ GeV [40].

The Minimal Supersymmetric Standard Model is a special case. In this model, the tree-level potential for the lightest Higgs boson is determined completely by supersymmetry. Radiative corrections to this potential are important. Nevertheless, it can be shown that $m_h < 130$ GeV in this model [41]. Here the conclusion is independent of any assumptions about grand unification.

4.3 The constraint on the Higgs mass from precision electroweak data

The previous two sections did not make any reference to the determination of the Higgs boson mass from the precision electroweak data. Those data give a second, independent argument for a light Higgs boson. The Higgs field contributes to electroweak observables through loop corrections to the W and Z propagators. The effect

is small, of order $\alpha \ln(m_h/m_W)$, but the accuracy of the measurements makes this effect visible. A fit of the current data to the Standard Model, using the measured value of the top quark mass, is consistent only if $\ln(m_h/m_W)$ is sufficiently small. The LEP Electroweak Working Group finds upper limits $m_h < 188$ GeV at the 95% CL and $m_h < 291$ GeV at the 99% CL [42]. Even using more conservative estimates of the theoretical errors [43], the limit on the Higgs boson mass is well within the range of a 500 GeV e^+e^- collider.

This Standard Model limit does not obviously apply to more general models of electroweak symmetry breaking. In what follows we will discuss its validity in various models. As previously, the result depends on whether or not the Higgs is fundamental.

We have noted in Section 4.1 that models with a fundamental Higgs boson typically satisfy decoupling. The practical effect of this is that, if new particles are sufficiently massive that they cannot be produced at LEP 2, their contributions to electroweak corrections are too small to affect the current global fits. In particular, fits to models of supersymmetry produce upper bounds on the Higgs mass similar to those from the Standard Model.

It is difficult to make a model with dynamical electroweak symmetry breaking that is consistent with precision electroweak measurements. The simplest technicolor models, for example, give several-percent corrections to electroweak observables [44,45,46]; effects this large are completely excluded. Even models with one $SU(2)$ doublet of techni-fermions give corrections of a size roughly double that for a 1000 GeV Higgs boson. With models of this type, it is typically necessary to invoke some mechanism that compensates the large corrections that appear in these models, and then to adjust the compensation so that the precision electroweak constraint is obeyed. In this process, the constraint on the Higgs boson mass can be relaxed.

A recent review [47] describes the three different compensation strategies that have been presented in the literature. One of these strategies leads to a lower value of the W mass and a larger Z width than predicted in the Standard Model. It can be distinguished by the improved precision electroweak measurements that we describe in Section 5.6. The other two strategies predict either new light particles with electroweak charge or other perturbations of Standard Model cross sections visible below 500 GeV. Thus, models based on new strong interactions can avoid having Higgs bosons below 500 GeV, but they predict phenomena observable at a 500 GeV linear collider.

4.4 The lightest supersymmetry partners are likely to appear at 500 GeV

For supersymmetric models of electroweak symmetry breaking, the arguments of the previous two sections give us confidence that we will be able to produce the lightest Higgs boson. But we also need to study the supersymmetry partners of quarks, leptons, and gauge bosons. Thus, we must also explore how heavy these particles are likely to be.

	$\tilde{\chi}_1^+$	\tilde{g}	\tilde{e}_R	\tilde{u}, \tilde{d}
Barbieri-Giudice [48]	110	350	250	420
Ross-Roberts [49]	110	560	200	520
de Carlos-Casas [50]	250	1100	450	900
Anderson-Castano [51]	270	750	400	900
Chan-Chattopadhyay-Nath [52]	250	930	550	900
Giusti-Romanino-Strumia [53]	500	1700	600	1700
Feng-Matchev-Moroi [54]	240/340	860/1200	1700/2200	2000/2300

Table 2.2: Upper limits on supersymmetry particle masses (in GeV) from the fine-tuning criterion found by various groups. In the last line, we have chosen two different breakpoints in fine-tuning from the results given in the paper.

Because supersymmetric generalizations of the Standard Model revert to the Standard Model when the superpartner masses are taken to be heavy, it is not possible to obtain upper limits on the masses of supersymmetric particles by precision measurements. One must take a different approach, related to the problems of the Standard Model discussed at the beginning of Section 4.1. As we noted there, it is a property of the Standard Model that radiative corrections from a high mass scale M contribute additively to the Higgs mass and vacuum expectation value, affecting m_W in the form

$$m_W^2 = \frac{g^2 v^2}{4} + \frac{\alpha}{\pi} M^2 + \dots . \quad (2.6)$$

It is possible to obtain a value of the W mass much less than M only if the various contributions cancel to high accuracy. For example, these terms must cancel to 3 decimal places for $M = 20$ TeV or to 30 decimal places for $M = 10^{18}$ GeV. Supersymmetry solves this problem by forbidding such additive corrections to m_W^2 . But this restriction applies only if supersymmetry is unbroken. If the masses of the superpartners are much greater than m_W , the fine-tuning problem returns.

This theoretical motivation leads us to expect that supersymmetric particles are most natural if they are light, of order a few hundred GeV. One can try to quantify this argument by limiting the amount of accidental cancelation permitted in the calculation of m_W . By now, many authors have studied this cancelation in a variety of supersymmetric models. In Table 2, we show the upper limits on supersymmetry particle masses found by seven groups for the parameter space of minimal gravity-mediated supersymmetry models (mSUGRA). The detailed calculations leading to these limits are different and, in many cases, involve conflicting assumptions. These differences are reflected in the wide variation of the limits on first- and second-generation slepton and squark masses evident in the table.

Nevertheless, these analyses are in general agreement about the required scale of the gaugino masses and (except for [53]) expect chargino pair production to be kinematically accessible at or near 500 GeV. A simplified but quantitative argument for this bound can be made [54] by writing the expression for m_W^2 in terms of the underlying parameters of the model, and eliminating these in terms of physical particle masses. For the representative value $\tan\beta = 10$, one finds

$$m_W^2 = -1.3\mu^2 + 0.3m^2(\tilde{g}) + \dots, \quad (2.7)$$

where the terms displayed involve the supersymmetric Higgs mass parameter and the gluino mass. The omitted terms involving scalar masses are more model-dependent. The gluino mass enters through its effect on the renormalization of the stop mass. For a gluino mass of 1 TeV, the requirement that the W mass is no larger than 80 GeV requires a fine-tuning of 1 part in 50. A similar level of fine-tuning is needed if μ is greater than 500 GeV.

As we will discuss in Section 5.2, the masses of the two charginos are closely related to the wino mass parameter m_2 and the Higgs mass parameter μ . In particular, the lighter chargino mass lies close to the smaller of these two values. The parameter m_2 is connected to the gluino mass in mSUGRA models by the grand unification relation

$$m_2/m(\tilde{g}) \approx \alpha_w/\alpha_s \approx 1/3.5. \quad (2.8)$$

This relation also holds in gauge-mediation, where, in addition, the masses of sleptons are predicted to be roughly the same size as the mass of the chargino. In other schemes of supersymmetry breaking, the chargino/gluino mass ratio can differ; for example, in anomaly-mediation, $m_2/m(\tilde{g}) \approx 1/8$. In all of these models, the bound on $m(\tilde{g})$ implies a strong bound on the lightest chargino mass. The fact that both m_2 and μ are bounded by the fine-tuning argument implies that there is also a bound on the mass of the heavier chargino. Indeed, one typically finds that the full set of chargino and neutralino states can be produced at an 800 GeV e^+e^- collider [54].

Although the fine-tuning limits are by no means rigorous, they indicate a preference for light supersymmetry partners. They encourage us to expect that we will be able to study the lighter chargino and neutralinos at the initial stage of the linear collider program, and all gauginos with a modest upgrade of the energy.

4.5 What if there is no fundamental Higgs boson?

Despite our arguments given in Section 4.1 for preferring a fundamental Higgs boson, electroweak symmetry breaking could result from a new strong interaction. Whereas for supersymmetry we have a well-defined minimal model, albeit one with many free parameters, here even the basic structure of the model is unknown and we will need more guidance from experiment. It is thus important to identify measurements that probe possible new strong interactions in a variety of ways.

In models with a composite Higgs boson, the Higgs mass can be large, 500 GeV or higher. If the Higgs is very heavy, there is no distinct Higgs resonance. A heavy but narrow Higgs boson can be studied at the LHC in its $Z^0 Z^0$ decay mode, and at a higher energy e^+e^- collider. A broad resonance or more general new strong interactions can be studied through WW scattering at TeV energies. This study can also be done at the LHC and at a higher energy linear collider [15]. However, in this case, the experiments are expected to be very challenging. Certain classes of models which are preferred by the arguments of Section 4.1 (*e.g.*, [32]) predict that no effect will be seen in these reactions.

In view of this, it is essential to have another way to probe models with a composite Higgs boson. This can be done by studying the effects of the new physics on the Standard Model particles that couple most strongly to it—the W , Z , and top quark. Because the Z couples to light fermions through a gauge current, effects of the new strong interactions are not expected to appear in Z decays, except possibly in $Z \rightarrow b\bar{b}$. The first real opportunity to observe these effects will come in the study of the W , Z , and t couplings. Effects of strong-interaction electroweak symmetry breaking can appreciably modify the Standard Model predictions for these couplings.

Without a specific model, it is difficult to predict how large these effects should be, but some estimates provide guidance. For example, triple gauge boson couplings can be related to parameters of the effective chiral Lagrangian describing the nonperturbative $SU(2) \times U(1)$ symmetry breaking. The parameter $\Delta\kappa_\gamma$ which contributes to the W anomalous magnetic dipole moment, is given by [15]

$$\Delta\kappa_\gamma = -2\pi\alpha_w(L_{9L} + L_{9R} + L_{10}) , \quad (2.9)$$

where the L_i are dimensionless parameters analogous to the Gasser-Leutwyler parameters of low energy QCD [55]. Naively putting in the QCD values, we find

$$\Delta\kappa_\gamma \sim -3 \times 10^{-3} . \quad (2.10)$$

A deviation of this size cannot be seen at LEP or the Tevatron. It is close to the expected error from the LHC. However, a 500 GeV e^+e^- collider can reach this sensitivity by the precision study of $e^+e^- \rightarrow W^+W^-$, as we will discuss in Section 5.5.

For the top quark, somewhat larger effects are expected, specifically in the $Z\bar{t}t$ coupling. As we noted in Section 4.1, it is already a problem for these models that the decay width for $Z \rightarrow b\bar{b}$ agrees with the Standard Model. However, models can contain several competing effects which add destructively in the $Z\bar{b}b$ coupling but constructively in the $Z\bar{t}t$ coupling [56,57,58]. In that case, 5–10% corrections to the $Z\bar{t}t$ coupling would be expected. These would produce corrections to the cross section for $e^+e^- \rightarrow t\bar{t}$ which would be observed through the measurement of this cross section at a 500 GeV e^+e^- collider. We will discuss the program of precision measurements of anomalous top quark couplings in Section 5.3.

In the past few years, there has been a theoretical preference for supersymmetry and other weakly-coupled models of electroweak symmetry breaking. If supersymmetric particles are not discovered at the LHC, this situation will change dramatically. In that case, anomalous W and t coupling measurements at an e^+e^- collider will be among the most central issues in high-energy physics.

4.6 What if the LHC sees no new physics?

Though we expect that the LHC will reveal a rich spectrum of new particles, it is possible that the LHC will see no new phenomena. How could the LHC see no sign of the interactions responsible for electroweak symmetry breaking? The LHC should not fail to find supersymmetry if it exists. The LHC, at full luminosity, should be sensitive to resonances in WW scattering beyond the limit set by s -channel unitarity. Thus, if the LHC fails to find signatures of electroweak symmetry breaking, it will not be because this collider does not have high enough energy. The scenarios in which the LHC fails—which, we emphasize, are very special scenarios occupying a tiny volume of typical parameter spaces—are those in which there is a light Higgs boson that does not have the decay modes important for detection at the LHC.

A Higgs boson with mass larger than about 150 GeV has a large production cross section from WW fusion and a substantial branching ratio to decay back to WW . Even if the hWW coupling is diluted as described below, it is hard for us to imagine that this signature will not be seen at the LHC.

But for Higgs bosons with mass below 150 GeV, it is possible that there are new particles with masses tuned so that their loop contributions to the $h\gamma\gamma$ coupling cancel the Standard Model contribution. This can happen, for example, at specific points in the parameter space of the Minimal Supersymmetric Standard Model [59]. It is also possible that a substantial fraction of the Higgs decays are to invisible final states such as $\tilde{\chi}_1^0\tilde{\chi}_1^0$. Finally, if there are several neutral Higgs fields, each of which has a vacuum expectation value, the strength of the squared hWW coupling for any individual field will be divided by the number of fields participating. Any of these three possibilities would compromise the ability of the LHC experiments to find and study the Higgs boson. The ability of an e^+e^- collider to see the Higgs boson does not depend on the Higgs decay pattern, but only on measurement of missing mass recoiling against a produced Z^0 boson. Thus, a 500 GeV e^+e^- collider would be the ideal instrument to study the Higgs boson under these special circumstances, as discussed in Section 5.1.

There is another way that the LHC could ‘discover nothing’ which we must confront. It could be that the Standard Model is correct up to a mass scale above 10^{16} GeV, and that the only new physics below that scale is one standard Higgs boson. This conclusion would be extremely vexing, because it would imply that the reason for the spontaneous breaking of electroweak symmetry and the values of the quark and lepton masses could not be understood as a matter of principle. In that case,

before giving up the quest for a fundamental theory, we should search in detail for non-standard properties of the observed Higgs boson. We will show in Section 5.1 that this study is ideally done at an e^+e^- linear collider. In this scenario, the mass of the Higgs boson must lie in a narrow window between 140 and 180 GeV, so an energy of 500 GeV would be sufficient. The final confirmation of the Standard Model would be compelling only after the Higgs boson has passed all of the precision tests possible at an e^+e^- collider.

5 Physics at a 500 GeV linear collider

We have argued in the previous section that there is a high probability that new physics associated with electroweak symmetry breaking will appear at a 500 GeV e^+e^- collider. We have given two different arguments that the Higgs boson should appear in e^+e^- annihilation at this energy. For models with TeV-scale supersymmetry, it is likely that the lighter chargino and neutralino states can also be found. For models with strong-coupling electroweak symmetry breaking, important precision measurements on the W , Z , and top quark can be made at these energies. In this section, we will describe these experiments and estimate the accuracy they can achieve for the realistic luminosity samples set out in Section 3.

To introduce this discussion, we should recall the advantageous features of e^+e^- collisions that have made them so useful in the past to provide a detailed understanding of the underlying physics. We will see that these features can also be used to great advantage in the experimental program for 500 GeV:

- The cross sections for new Standard Model and exotic processes, and those of the dominant backgrounds, are all within about 2 orders of magnitude of one another (see Fig. 2.1). Thus, the desired signals have large production rates and favorable signal to background ratios. This situation contrasts with that at hadron colliders, where the interesting signals are typically very tiny fractions of the total cross section.
- Most of the interesting processes have simple two-body kinematics, from an initial state with well-defined quantum numbers.
- The cross sections for these processes are due to the electroweak interactions and can be predicted theoretically to part per mil accuracy.
- These processes also have known total energy and momentum at the level of the parton-parton interaction, with well understood and measurable smearing from initial-state radiation and beamstrahlung.

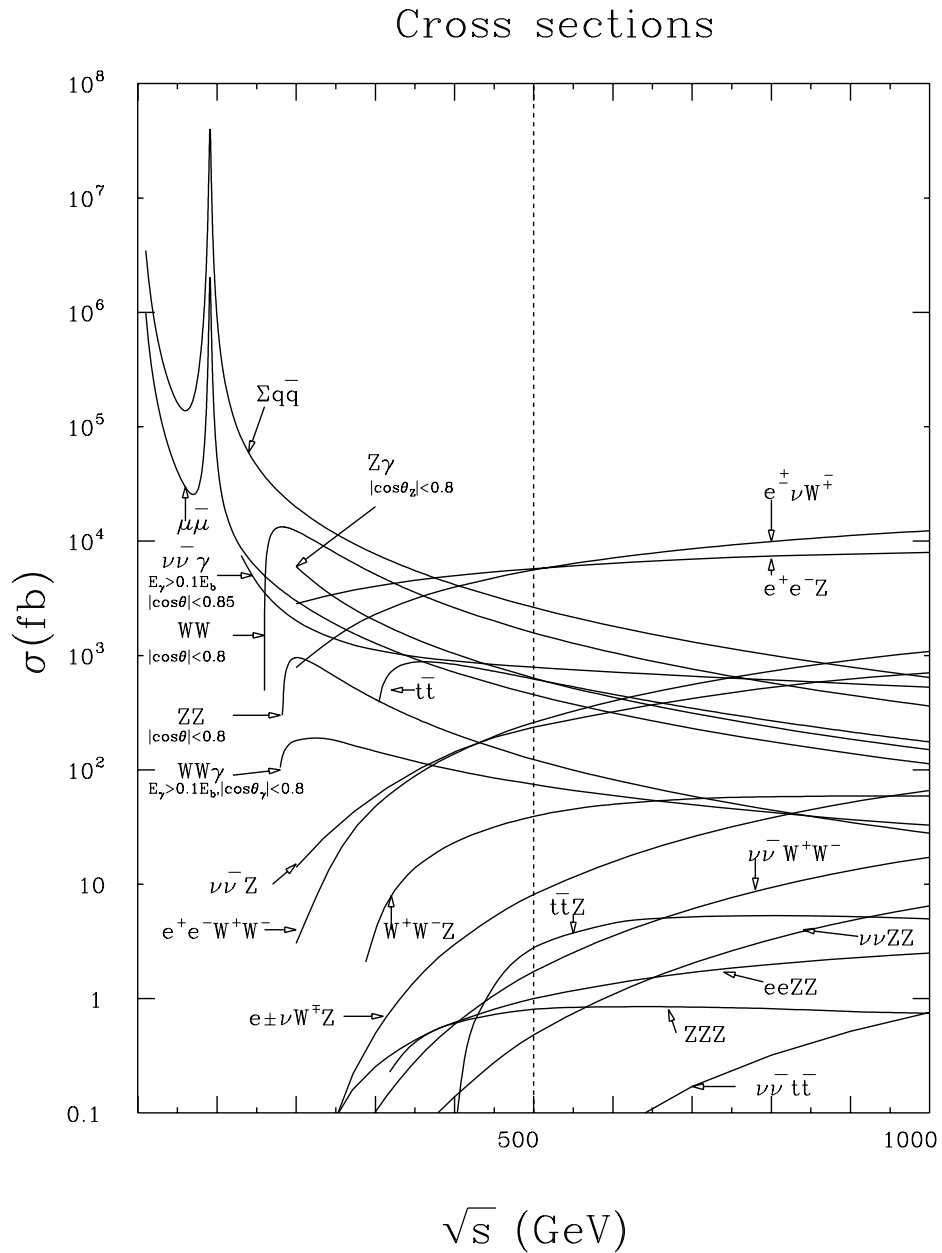


Figure 2.1: Cross sections for a variety of physics processes at an e^+e^- linear collider, from [60].

- The electron beam may be polarized, allowing selective suppression of backgrounds, separation of overlapping signals and measurement of parity-violating couplings.
- The collider energy may be varied to optimize the study of particular reactions.

These features of e^+e^- collisions allow the study of heavy particles and their decays in many difficult circumstances, including detection of decays that are rare or have less distinct signatures, measurement of particle masses when some decays are invisible, measurement of spin, parity, CP, and electroweak quantum numbers, measurement of widths and coupling constants, and measurement of mixing angles.

An extensive program studying physics at future high energy e^+e^- colliders has been carried out over the past few years as a collaborative effort of scientists in Europe, Asia, and America. In this section and the next, we will report on some highlights of that program. Much more detail on all of these studies can be found from the reviews [1,2,3,4].

5.1 Study of the Higgs boson

The Higgs boson plays the central role in electroweak symmetry breaking and the generation of masses for quarks, leptons, and vector bosons. In the Standard Model, the Higgs boson is a simple scalar particle which couples to each fermion and boson species proportionately to its mass. Higher-order processes which couple the Higgs boson to gg , $\gamma\gamma$, and γZ^0 add richness to its phenomenology. If the Standard Model is not correct, the surprises could come at many different points. Several scalar bosons could have large vacuum expectation values and thus could share responsibility for the W and Z masses. Different scalar bosons could be responsible for the up- and down-quark masses, or a different boson could produce the masses of third-generation fermions. These deviations from the standard picture might be large effects, or they might appear only in precision measurements.

One of the most remarkable features of the experimental environment of the linear collider is its ability to probe these issues directly. Each piece of information—from cross sections, angular distributions, and branching ratios—connects directly to a fundamental coupling of the Higgs particle. In this section, we will review how measurements at a linear collider can assemble a complete phenomenological profile of the Higgs boson.

It is almost certain that the Higgs boson will have been discovered before the linear collider begins operation. Results from LEP 2 presently imply that $m_h \geq 108$ GeV at the 95% confidence level [42]. It is expected that this limit will go up to about 115 GeV as LEP 2 reaches its maximum energy. The Tevatron may be able to discover a Higgs boson up to about 180 GeV [61]. This already covers most of the range of Higgs boson masses favored by the arguments of Section 4.

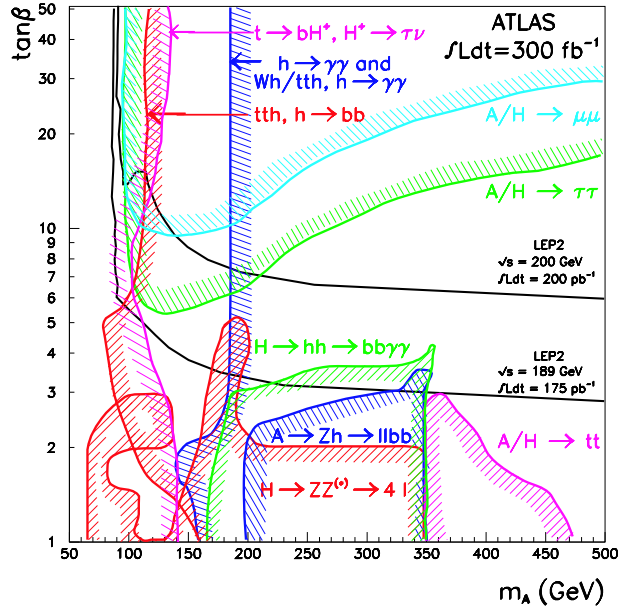


Figure 2.2: Capability of the ATLAS experiment to study the Higgs sector of the MSSM [62].

The LHC studies have shown that a Higgs boson with the properties expected in the Standard Model can be discovered at that facility for any value of its mass. In addition, in models with an extended Higgs sector—for example, the Minimal Supersymmetric Standard Model—the LHC should be able to find one and possibly several of the Higgs particles. A recent summary of the LHC sensitivity to various MSSM Higgs processes is shown in Fig. 2.2. There are some regions of parameter space for which only one channel can be observed; in any case, it is typical that considerable luminosity is required for positive observation. In Section 4.6, we have noted some specific scenarios in which it is difficult to find the Higgs boson at the LHC. But, more generally, the LHC is limited in its ability to assemble a complete picture of the Higgs boson properties by the fact that Higgs boson production is such a tiny fraction of the LHC cross section that the Higgs particle must be reconstructed in order to study its production and decay.

5.1.1 Discovery of the Higgs independent of its decay modes

As a first step, we will argue that the Higgs boson can be found at a linear collider whatever its decay scheme might be. It is not necessary to reconstruct a Higgs boson to discover the particle or to measure its coupling to the Z^0 . At low energies, the

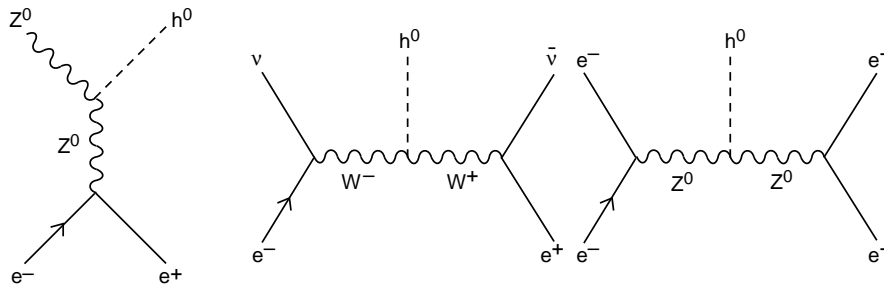


Figure 2.3: Processes for production of the Higgs boson at an e^+e^- linear collider.

dominant Higgs production process in e^+e^- collisions is $e^+e^- \rightarrow Z^0h^0$, shown as the first diagram in Fig. 2.3. If the Z^0 is reconstructed from any one of its well-known decay modes, the Higgs is seen as a peak in the missing mass distribution recoiling against the Z^0 . This detection is independent of the Higgs decay mode, visible or invisible. Simulations show that this process is very clean, with minimal backgrounds. Figure 2.4 shows the expected signal of the Higgs boson using lepton, neutrino, and hadronic Z decays for a 30 fb^{-1} event sample [63].

The cross section for Z^0h^0 production depends on the magnitude of the ZZh coupling. Thus, the observation of the Higgs boson in this process measures the size of that coupling. If we replace the Higgs field h^0 by its vacuum expectation value, we see that this same coupling generates the mass of the Z through the Higgs mechanism. Thus, determination of the absolute magnitude of the cross section for $e^+e^- \rightarrow Z^0h^0$ tests whether the observed h^0 generates the complete mass of the Z^0 . Since Higgs measurements at the LHC require reconstruction of the Higgs boson, the LHC experiments can only measure ratios of couplings and cannot determine the ZZh coupling directly.

If there are several Higgs bosons contributing to the mass of the Z^0 , the e^+e^- cross section for production of the lightest Higgs will be smaller, but heavier Higgs bosons must appear at higher values of the recoil mass. To discuss this quantitatively, let the coupling of the boson h_i be g_{ZZi} . (For simplicity, we assume that all of the h_i are $SU(2)$ doublets; this assumption can be checked by searching for multiply-charged Higgs states.) Then the statement that the sum of the contributions from the vacuum expectation values of the h_i generates the full mass of the Z^0 can be expressed as the sum rule [64]

$$\sum_i g_{ZZi}^2 = 4m_Z^4/v^2, \quad (2.11)$$

where $v = 246 \text{ GeV}$. With a 200 fb^{-1} event sample at 500 GeV, Higgs particles h_i can be discovered in recoil against the Z^0 down to a cross section of 0.2 of the Standard Model value for $m(h_i) = 350 \text{ GeV}$, and below 0.01 of the Standard Model value for $m(h_i) = 150 \text{ GeV}$ [3]. If all contributing Higgs bosons have masses below 150

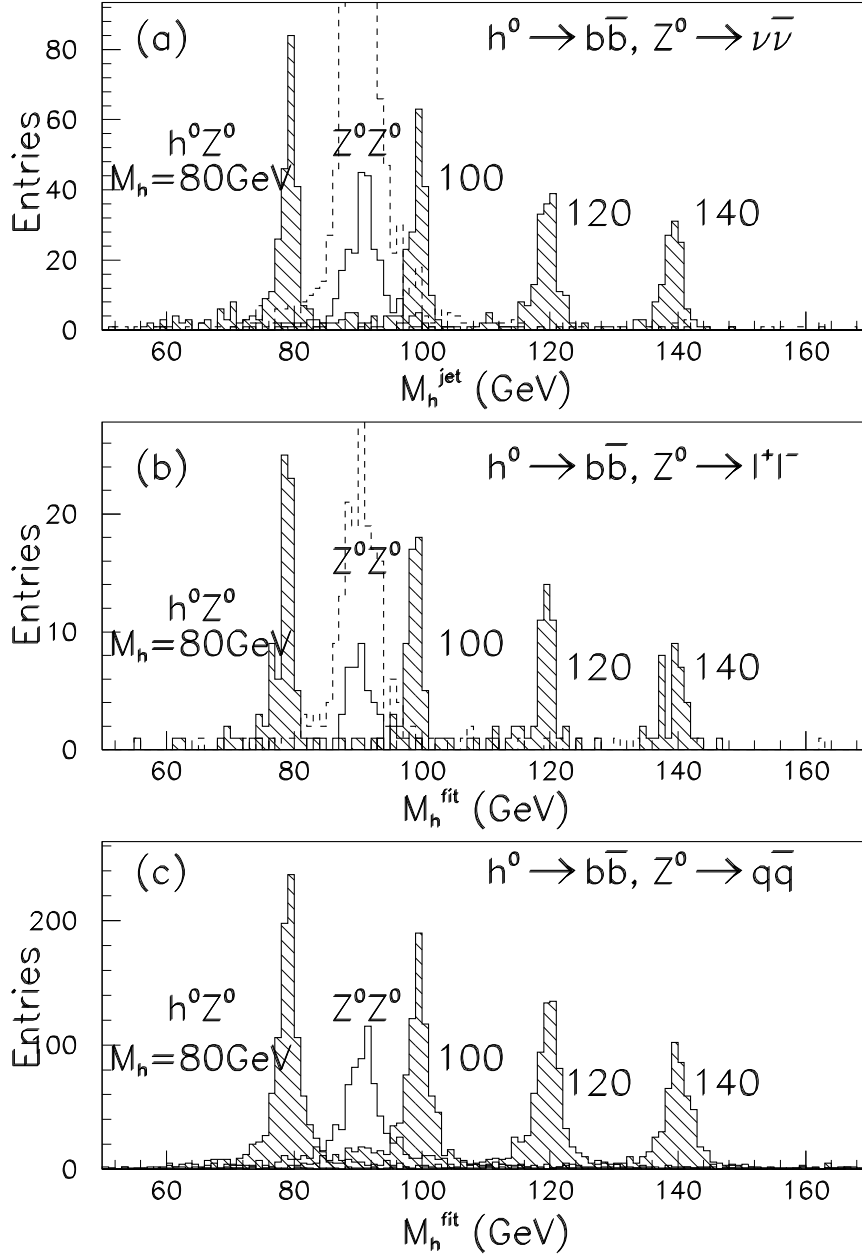


Figure 2.4: Higgs reconstruction in the process $e^+e^- \rightarrow Z^0h^0$ for various Higgs boson masses, using $\ell^+\ell^-$, $\nu\bar{\nu}$, and hadronic Z^0 decays, for a 30 fb^{-1} event sample at 300 GeV, from [63]. The background is dominated by the process $e^+e^- \rightarrow Z^0Z^0$, which produces the missing-mass peak at m_Z . The unshaded solid histogram gives the background if a b -tag is applied to the Higgs candidate. The dashed histograms in (a) and (b) show the background with no b -tag.

GeV, the sum rule can be checked in a 200 fb^{-1} experiment to 5% accuracy, with dominantly statistical uncertainty. When we have saturated the sum rule (2.11), we will have discovered all of the Higgs states that contribute to the Z^0 mass.

5.1.2 Measurement of the Higgs branching ratios

The Higgs boson branching ratios are crucial indicators of nature of this particle, and of possible extensions beyond the Standard Model. The LHC can only make rough measurements of these, to about the 25% level, and only for some values of the Higgs boson mass [62,65]. Once the mass is known, it is straightforward at the linear collider to measure Higgs boson absolute branching fractions into two fermion or two gauge bosons for any of the production processes of Fig. 2.3 using the energy and momentum constraints. All decay modes of the Z^0 can be used in this study, even $Z^0 \rightarrow \nu\bar{\nu}$ (20% of the Z^0 total width) [66].

Methods for determining the Higgs cross sections to various decay channels have been studied recently in [66]. It is straightforward that the $b\bar{b}$ decays can be identified by vertex tagging. The studies show that $c\bar{c}$ decays can also be identified by vertex tagging with high efficiency, since the first layer of a vertex detector can be placed at about 1 cm from the interaction point. Multi-jet decays of the h^0 are typically WW^* . Table 3 gives a summary of the precision expected for a large variety of decay modes for the case of a 120 GeV Higgs boson. This case is especially favorable in terms of the number of final states which are accessible, but it is also the value of the Higgs mass which is most probable in the Minimal Supersymmetric Standard Model. Expectations for Higgs branching ratio measurements at other values of the Higgs mass (assuming 500 fb^{-1} at 350 GeV) are shown in Fig. 2.5 [66]. If the Standard Model Higgs mass approaches 200 GeV, the dominance of the WW and ZZ decays will render the fermionic decays progressively more difficult to observe.

The Higgs branching ratios directly address the question of whether the Higgs boson generates the masses of all Standard Model particles. If the vacuum expectation value of h^0 produces the fermion masses, the couplings of h^0 to b , c , and τ should be simply determined from the ratio of their masses. Similarly, the coupling of the h^0 to WW or, for the case of a light Higgs, to one on-shell and one off-shell W , measures the fraction of the W mass due to the Higgs vacuum expectation value.

The Minimal Supersymmetric Standard Model includes an extended Higgs sector with two $SU(2)$ doublets. For the most general case of a two-Higgs-doublet model, vacuum expectation values of both Higgs fields contribute to the quark, lepton, and boson masses and the predictions for branching ratios differ qualitatively from those in the Standard Model. However, in the MSSM with heavy superpartners, one scalar boson H^0 is typically heavy and the orthogonal boson h^0 , which must be light, tends to resemble the Higgs boson of the Standard Model. For example, the ratio of branching

		200 fb ⁻¹	500 fb ⁻¹
$\Delta\sigma_{ZH}/\sigma_{ZH}$		4%	3%
$\Delta\sigma_{H\nu\nu}BR(b\bar{b})/\sigma_{H\nu\nu}BR(b\bar{b})$		3%	2%
$\Delta BR/BR$	$b\bar{b}$	3%	2%
	WW^*	8%	5%
	$\tau^+\tau^-$	7%	6%
	$c\bar{c}$	10%	8%
	gg	8%	6%
	$\gamma\gamma$	22%	14%

Table 2.3: Expected errors in branching ratio and coupling measurements for a Standard Model Higgs boson of mass 120 GeV, from measurements at 350 GeV.

ratios to $b\bar{b}$ and WW^* is corrected by the factor

$$1 + 2 \cos^2 2\beta \sin^2 2\beta \frac{m_Z^2}{m_H^2} + \dots \quad (2.12)$$

Nevertheless, accurate branching ratio measurements can distinguish the MSSM Higgs boson from the Standard Model Higgs boson over a large region of parameter space. From the results of [66], the 500 fb⁻¹ experiment discussed above would exclude corrections from the MSSM Higgs structure for m_A up to at least 550 GeV. The linear collider determination of branching ratios is sufficiently accurate that the theoretical uncertainty in the charm quark mass is actually the dominant source of error. New approaches to the determination of the quark masses in lattice gauge theory should give more accurate values in the next few years [67] and thus improve the power of this measurement.

5.1.3 Measurement of the Higgs boson width

It will be critical to know the total width of the Higgs, Γ_{tot} , accurately. For a Higgs boson mass below 200 GeV, the total width is expected to be below 1 GeV, too small to be measured at the LHC or directly at the linear collider. To determine this width, one will need to combine an absolute measurement of a decay rate or coupling constant with the measurement of the branching ratio for the corresponding channel. The most promising method is to use the branching ratio to WW^* . The absolute size of the WW^*h coupling can be determined either from the $SU(2) \times U(1)$ relation $g_{WW^*h}^2/g_{ZZh}^2 = \cos^2 \theta_w$ or, in a more model-independent way, from the cross section for h^0 production by the WW fusion process shown as the second diagram

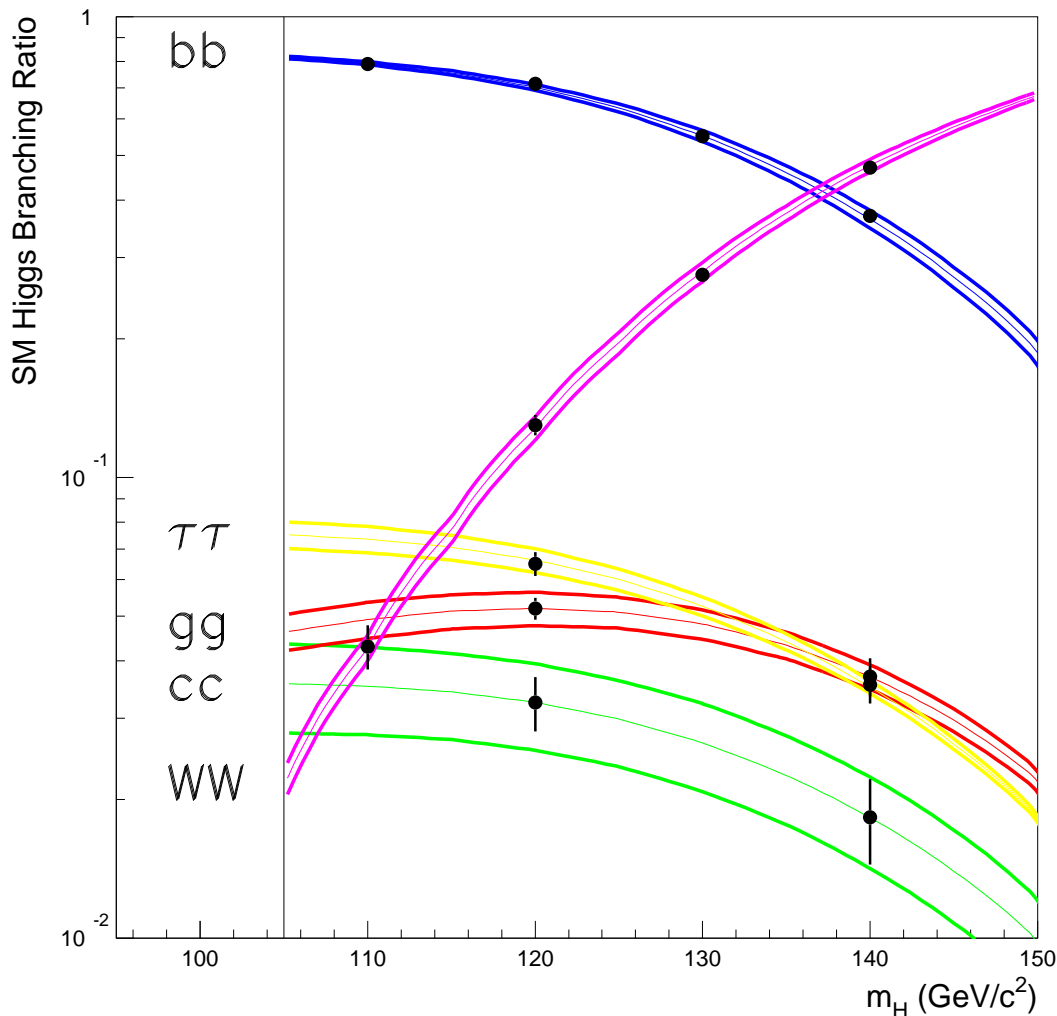


Figure 2.5: Determination of Higgs boson branching ratios in a variety of decay modes, from [66]. The error bars show the expected experimental errors for 500 fb^{-1} at 350 GeV. The bands show the theoretical errors in the Standard Model predictions.

in Fig. 2.3. (The ZZ fusion process is expected to add only a small contribution.) From Table 3, the Higgs branching ratio to WW^* gives the dominant source of error in this measurement.

If the $\gamma\gamma$ collider option is realized by backscattering polarized laser light off the e^\pm beams, then the process $\gamma\gamma \rightarrow h^0$ can be used to measure the absolute partial width $\Gamma(h^0 \rightarrow \gamma\gamma)$. This width, which can be determined to about 5% accuracy with

a 200 fb⁻¹ dedicated experiment [68], is of great interest in its own right, since it measures a sum of contributions from all heavy charged particles that couple to the h^0 .

5.1.4 Measurement of the spin-parity and CP of the Higgs boson

It will be essential to determine the quantum numbers of an observed Higgs boson unambiguously. The LHC can rule out spin 1 if the decay $H \rightarrow \gamma\gamma$ is observed. If the decay $H \rightarrow ZZ$ is observed, spin 0 and 1 could be distinguished at the LHC, but the CP quantum numbers will be difficult to determine in any case. The linear collider will thus be needed to determine the Higgs quantum numbers.

If the Higgs field has a vacuum expectation value, it must be a CP-even spin-0 field. Thus, a Higgs boson produced in $e^+e^- \rightarrow Z^0 h^0$ with a rate comparable to the Standard Model rate must have these quantum numbers. However, there are a number of checks on these properties that are available from the kinematics of Higgs production. In the limit $s \gg m_Z^2, m_h^2$, a scalar Higgs boson produced in this reaction has an angular distribution

$$\frac{d\sigma}{d\cos\theta} \sim \sin^2\theta \quad , \quad (2.13)$$

and the Z^0 recoiling against it is dominantly longitudinally polarized, and so that distribution in the decay angle peaks at central values. (For a CP-odd scalar, these distributions differ qualitatively.) If the center of mass energy is not asymptotic, the corrections to these relations are predicted from kinematics. For example, Fig. 2.6 shows a simulation of the angular distribution at 300 GeV and a comparison to the distribution expected for a Higgs scalar.

The production of the Higgs boson in $\gamma\gamma$ collisions goes through a loop diagram which can give both scalar and pseudoscalar couplings. Thus, the $\gamma\gamma$ collider option offers a nontrivial test of CP violation. With longitudinal γ polarization, the asymmetry of Higgs production cross sections

$$A_\gamma = \frac{\sigma(\gamma_L\gamma_L) - \sigma(\gamma_R\gamma_R)}{\sigma(\gamma_L\gamma_L) + \sigma(\gamma_R\gamma_R)} \quad (2.14)$$

vanishes for pure scalar or pseudoscalar coupling to $\gamma\gamma$ but is nonzero if the Higgs is a mixture of CP eigenstates. Models with CP violation in the top sector can give 10% or larger asymmetries [70]. In models with extended Higgs sectors, this polarization asymmetry can incisively separate the heavy scalar and pseudoscalar Higgs resonances [71].

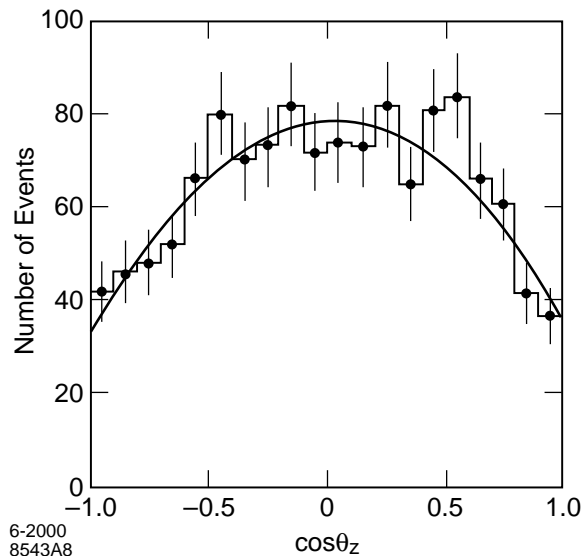


Figure 2.6: Angular distribution of the Z boson in $e^+e^- \rightarrow Z^0h^0$, as reconstructed from a 50 fb^{-1} event sample at 300 GeV, from [69].

5.1.5 Measurement of the Higgs self couplings

The Higgs self-couplings are uniquely fixed in the Standard Model in terms of the Higgs field expectation value v ; in the minimal supersymmetric model, they depend on the Higgs field couplings and mixings. Measuring the self-couplings is a crucial step in checking the consistency these models, and it gives added information on the parameters of supersymmetric models. It appears that observation of Higgs pair production at the LHC will be very difficult due to the dominance of gluon fusion production and large QCD backgrounds [72]. In e^+e^- collisions, production of two Higgs bosons in the final state can occur for any of the diagrams of Fig. 2.4 by radiating an additional Higgs from any of the gauge boson legs, or through the trilinear Higgs coupling. The cross sections for production of a pair of Higgs bosons with an associated Z boson have been calculated to be of order 0.5 fb for $m_h = 110 \text{ GeV}$ at $\sqrt{s} = 500 \text{ GeV}$ in the Standard Model [73]. Cross sections for various supersymmetric Higgs pair-production processes are comparable for much of the supersymmetric parameter space. The final state of Zhh , with both Higgs bosons observed as $b\bar{b}$, should provide a detectable signature without large backgrounds, yielding a precision on the trilinear Higgs coupling of roughly 25% for 600 fb^{-1} .

5.2 Studies of supersymmetry

In Section 4, we argued that the new physics at the TeV energy scale is likely to be a supersymmetric extension of the Standard Model. If supersymmetric particles

appear at the next step in energy, they will provide a rich field for experimental study. This study will address two separate and important issues. First, supersymmetry entails a fundamental modification of the structure of space-time. Supersymmetry can be described as the statement that spinors and fermions are an integral part of space-time geometry, or, alternatively, that there are new space-time dimensions which are fermionic in character. It requires new gravitational equations that include a spin- $\frac{3}{2}$ partner of the graviton. If we are to claim that Nature has this structure, we must to prove it experimentally by demonstrating the quantum number assignments and symmetry relations that this structure requires.

Second, phenomenological models with supersymmetry introduce a large number of new physical parameters. The masses of supersymmetric particles, and other parameters associated with spontaneous supersymmetry breaking, are not fixed from currently known principles but, rather, must be determined experimentally. The most general description of supersymmetry breaking even in the ‘Minimal’ Supersymmetric Standard Model contains 105 parameters. Each explicit model of spontaneous supersymmetry breaking gives predictions for these parameters or relations among them. But there is no ‘Standard Model’ of supersymmetry breaking. In the literature, one finds at least three general approaches—gravity-, gauge-, and anomaly-mediation—each of which has numerous variants. Each approach is derived from assumptions about new physics at a higher energy scale, which ranges from 10^5 to 10^{19} GeV depending on the model. The various models predict mass spectra and mixing parameters that differ characteristically. These observables provide clues to the nature of physics at extremely short distances, possibly even to the truly fundamental physics at the scale of grand unification or quantum gravity [74].

Supersymmetric particles may well be discovered in Run II of the Tevatron. In any case, if supersymmetry is relevant to electroweak symmetry breaking, supersymmetric particles should surely be found at the LHC. The LHC collaborations have demonstrated that they would be sensitive to quark and gluon superpartners up to masses of at least 2 TeV. For the gluino, this reach goes about a factor of 2 beyond the fine-tuning limits given in Table 2. Reactions which produce the squarks and gluinos also produce the lighter supersymmetric particles into which they decay. The ATLAS and CMS collaborations have presented some striking analyses at specific points in the parameter space of mSUGRA models in which 3 to 5 mass parameters can be determined from kinematics. From this information, the four parameters of the mSUGRA model can be determined to 2–10% accuracy [62,75].

Ultimately, though, hadron colliders are limited in their ability to probe the underlying parameters of supersymmetric models. Because the LHC produces many SUSY particles and observes many of their decay chains simultaneously, it is difficult to isolate parameters and determine them in a model-independent way. It is difficult to determine the spin and electroweak quantum numbers of particles unambiguously. And, only limited information can be obtained about the heavier color-singlet

particles, including sleptons and heavier charginos and neutralinos, and about the unobserved lightest neutralino.

It is just for these reasons that one needs a facility that can approach the spectroscopy of supersymmetric particles from an orthogonal direction. An e^+e^- collider can study supersymmetric particles one at a time, beginning with the lightest and working upward to particles with more complex decay patterns. For each particle, the measurements go well beyond simple mass determinations. We will give a number of illustrative examples in this section.

To carry out these measurements, it is only necessary that supersymmetric particles can be pair-produced at the energy provided by the e^+e^- collider. In the program that we have presented in Section 2, in which a collider with an initial energy of 500 GeV evolves to higher center of mass energies, one can eventually create the full set of supersymmetry particles. Here we concentrate on the expectations for 500 GeV. In Section 4.4, we have argued that the lightest charginos and neutralinos, the supersymmetric partners of the photon, W , Z , and Higgs bosons, should be produced already at the initial 500 GeV stage. The mSUGRA models discussed in Section 4.4 do not place such strong constraints on the masses of lepton superpartners, but in other schemes of supersymmetry breaking, such as gauge-mediation and the no-scale limit of gravity-mediation, it is natural for the sleptons to be as light as the charginos. Because the experimental study of sleptons is conceptually very simple, we will present the linear collider experimental program for sleptons in this section along with our discussion of charginos. Other issues for the experimental study of supersymmetry will be discussed in Section 6.2.

Our discussion of the basic supersymmetry measurements in this section will be rather detailed. In reading it, one should keep in mind that the linear collider offers a similar level of detailed information for any other new particles that might appear in its energy range.

5.2.1 Slepton mass measurement

The simple kinematics of supersymmetric particle pair production allows direct and accurate mass measurements. The technique may be illustrated with the process of pair production and decay of the $\tilde{\mu}_R^-$, the scalar partner of the μ_R^- . The process $e^+e^- \rightarrow \tilde{\mu}_R^- \tilde{\mu}_R^+$ produces the sleptons at a fixed energy equal to the beam energy. The $\tilde{\mu}_R^-$ is expected to decay to the unobserved lightest neutralino via $\tilde{\mu}_R^- \rightarrow \mu^- \tilde{\chi}_1^0$. Then the final muons are distributed in energy between kinematic endpoints determined by the masses in the problem. Since the $\tilde{\mu}_R^-$ is a scalar, the distribution of muons is isotropic in the $\tilde{\mu}_R^-$ rest frame and flat in energy in the lab frame. Thus, the observed energy distribution of muons has the shape of a rectangular box, and the masses of both the $\tilde{\mu}_R^-$ and the $\tilde{\chi}_1^0$ can be read off from the positions of the edges.

In measuring slepton pair production in e^+e^- collisions, special attention must be

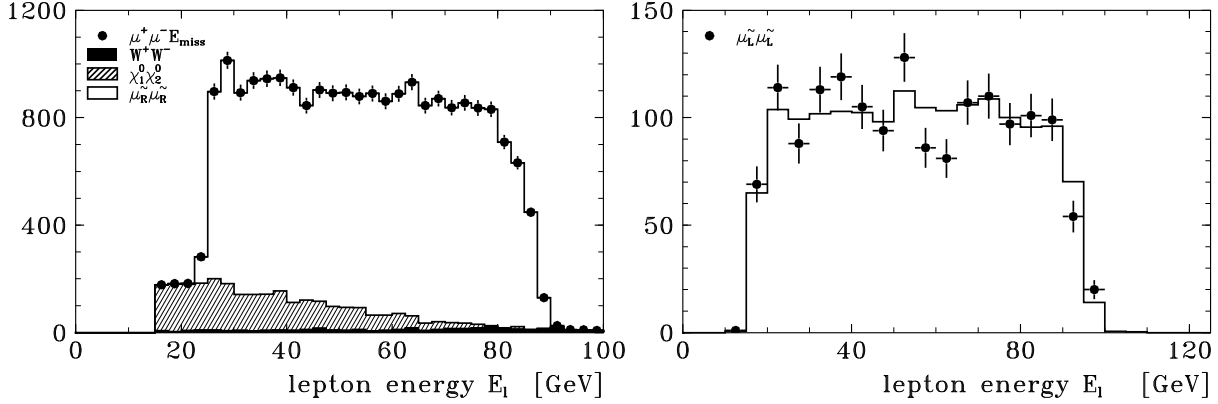


Figure 2.7: Energy distribution of muons resulting from processes $e^+e^- \rightarrow \tilde{\mu}^- \tilde{\mu}^+$, followed by $\tilde{\mu}$ decay, from [77]. left: $e^+e^- \rightarrow \tilde{\mu}_R^- \tilde{\mu}_R^+$, for a 160 fb^{-1} event sample at 320 GeV; right: $e^+e^- \rightarrow \tilde{\mu}_L^- \tilde{\mu}_L^+$, with selection of $\tilde{\mu}_L \rightarrow \mu \tilde{\chi}_2^0$, $\tilde{\chi}_2^0 \rightarrow \ell^+ \ell^- \tilde{\chi}_1^0$ decays on both sides, for a 250 fb^{-1} event sample at 500 GeV. The electron beam polarization is used to reduce the background from $e^+e^- \rightarrow W^+W^-$.

paid to the backgrounds from two-photon processes in which the primary scattered electrons are undetected within the beam pipes. This makes it important for the detector to have good coverage at forward and backward angles. It may be useful for gaining further control over this process to provide tagging detectors at very small angles [76].

On the left side of Fig. 2.7, we show simulation results for $\tilde{\mu}_R$ pair production [77]. The dominant background (shaded in the figure) comes from other supersymmetry processes. The rounding of the rectangle on its upper edge is the effect of beamstrahlung and initial state radiation. The simulation predicts a measurement of both the $\tilde{\mu}_R^-$ and the $\tilde{\chi}_1^0$ masses to 0.2% accuracy. The right side of Fig. 2.7 shows the muon energy distribution from pair production of the $\tilde{\mu}_L^-$, the partner of the μ_L^- . Decays of the form $\tilde{\mu}_L \rightarrow \mu \tilde{\chi}_2^0$, $\tilde{\chi}_2^0 \rightarrow \ell^+ \ell^- \tilde{\chi}_1^0$ are selected on both sides of the event to obtain a very clean 6 lepton signature. Despite the low statistics from the severe event selection, this analysis also gives the $\tilde{\mu}_L^-$ and the $\tilde{\chi}_2^0$ masses to 0.2% accuracy. At the LHC, the mass of the lightest neutralino $\tilde{\chi}_1^0$ typically cannot be determined directly, and the masses of heavier superparticles are determined relative to the $\tilde{\chi}_1^0$ mass. So not only do the e^+e^- measurements provide model-independent slepton masses, they also provide crucial information to make the superpartner mass measurements from the LHC more model-independent.

The same strategy can be applied to determine the masses of other superpartners. Examples with sneutrinos, scalar top, and charginos are shown in [78]. Even higher

accuracies can be obtained by scanning the e^+e^- cross section near each pair production threshold. This costs about 100 fb^{-1} per threshold, but it allows particle mass measurements to better than 1 part per mil [77].

5.2.2 Slepton properties

An e^+e^- collider can not only measure the masses of superparticles but also can determine many more properties of these particles, testing predictions of supersymmetry from the most qualitative to the most detailed.

Before anything else, it is important to verify that particles that seem to be sleptons are spin 0 particles with the Standard Model quantum numbers of leptons. A spin 0 particle has a characteristic angular distribution in e^+e^- annihilation, proportional to $\sin^2\theta$. Even though there are missing neutralinos in the final state of $e^+e^- \rightarrow \tilde{\mu}^- \tilde{\mu}^+$, there are enough kinematic constraints that the angular distribution can be reconstructed [79]. The magnitude of the cross section can be computed for each electron polarization with typical electroweak precision; it depends only on the Standard Model quantum numbers of the produced particle and thus determines these quantum numbers.

A major issue in supersymmetry is the flavor-dependence of supersymmetry breaking parameters. Using the endpoint technique above, the selectron and smuon masses can be compared at a level below the 1 part per mil level. It is somewhat more difficult to study the superpartners of the τ , but even in this case the masses can be found to percent accuracy by locating the endpoint of the energy distribution of stau decay products [80].

It is typical in supersymmetry scenarios with large $\tan\beta$ that the superpartners of τ_R^- and τ_L^- mix, and that the lighter mass eigenstate is actually the lightest slepton. If the mass difference between the lighter stau and the other leptons is significant, this can create a problem for the study of supersymmetry at LHC, since then supersymmetry decay cascades typically end with τ production. A parameter point studied by the ATLAS supersymmetry group illustrates the problem [62]. We have just noted that there is no difficulty in measuring the stau masses at a linear collider. In addition, since the production cross section depends only on electroweak quantum numbers, it is possible to determine the mixing angle from total cross section and polarization asymmetry measurements. The characteristic dependence of the polarization asymmetry on the stau mixing angle is shown in Fig. 2.8. The final state τ polarization provides another diagnostic observable which can be used to analyze the composition of the stau or of the neutralino into which it decays [80].

The cross section for production of the electron partners is somewhat more complicated, because this process can proceed both by e^+e^- annihilation and by the exchange of neutralinos, as shown in Fig. 2.9. In typical models, the dominant contribution actually comes from exchange of the lightest neutralino. Thus, the selectron

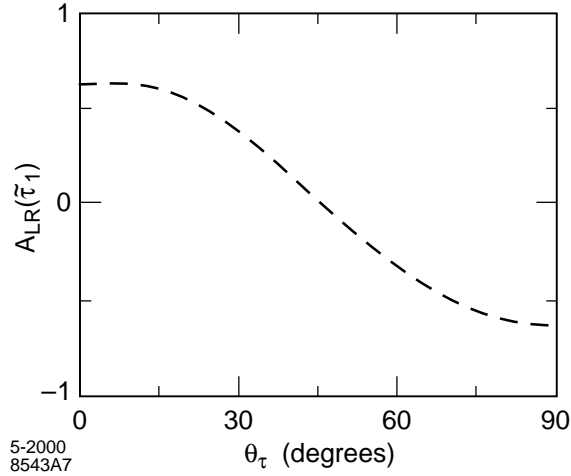


Figure 2.8: Polarization asymmetry of $e^+e^- \rightarrow \tilde{\tau}_1^+ \tilde{\tau}_1^-$ as a function of the stau mixing angle.

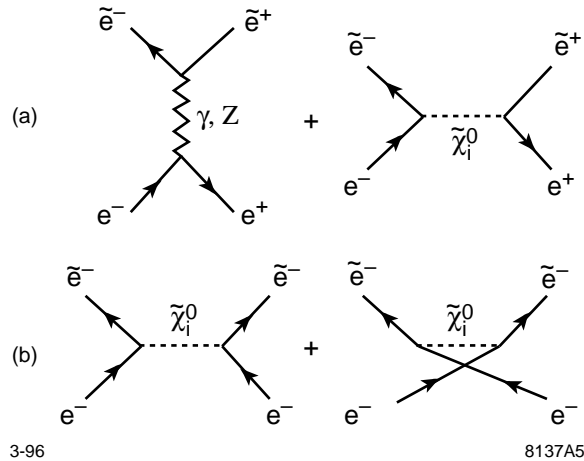


Figure 2.9: Diagrams contributing to selectron pair production: (a) $e^+e^- \rightarrow \tilde{e}^+ \tilde{e}^-$, (b) $e^-e^- \rightarrow \tilde{e}^- \tilde{e}^-$.

production cross section can give further information on the mass and the properties of this particle. The study of neutralinos is complicated by the fact that the various neutralino species can mix. In the Section 5.2.4, we will discuss this mixing problem and present methods for resolving it experimentally using e^+e^- data on chargino production. Neutralino mixing can also be studied in selectron pair production; an illustrative analysis is given in [79].

Once the mixing of neutralinos is understood, the selectron pair production can test the basic idea of supersymmetry quantitatively, by testing the symmetry relation of coupling constants. For simplicity, consider a model in which the lightest neutralino

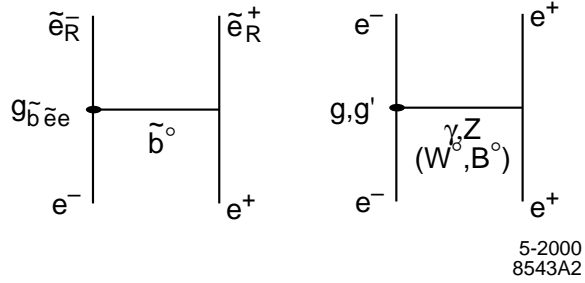


Figure 2.10: Comparison of the weak interaction coupling g' and its supersymmetric counterpart $g_{\tilde{b}\tilde{e}e}$.

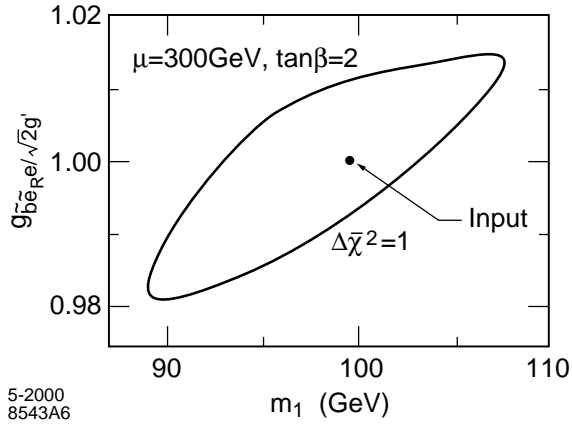


Figure 2.11: Determination of the $g_{\tilde{b}\tilde{e}e}$ coupling from a 100 fb^{-1} measurement of selectron pair production, from [80].

is the superpartner \tilde{b} of the $U(1)$ gauge boson of the Standard Model, and imagine comparing the processes of \tilde{e}_R pair production and Bhabha scattering, as illustrated in Fig. 2.10. By supersymmetry, the coupling constant at the $e\tilde{e}\tilde{b}$ vertex must be simply related to the $U(1)$ electroweak coupling: $g_{\tilde{b}\tilde{e}e} = \sqrt{2}g'$. A measurement of the forward cross section for $e^+e^- \rightarrow \tilde{e}_R^+\tilde{e}_R^-$ can give a precision test of this prediction.

Detailed simulation of selectron pair production has shown that the ratio $g_{\tilde{b}\tilde{e}e}/\sqrt{2}g'$ can be measured to a precision of about 1%, as shown in Fig. 2.11 [80]. (This analysis uses data from the same cross section measurement both to fix the parameters of the neutralino mixing and to determine $g_{\tilde{b}\tilde{e}e}$.) Even higher accuracy can be achieved by studying selectron production in e^-e^- collisions. The ratio $g_{\tilde{W}\tilde{\nu}e}$ can also be determined from chargino pair production and compared to its Standard Model counterpart to about 2% accuracy. At these levels, the measurement would not only provide a stringent test of supersymmetry as a symmetry of Nature, but also it might be sensitive to radiative corrections from heavy squark and slepton species [81,82,83].

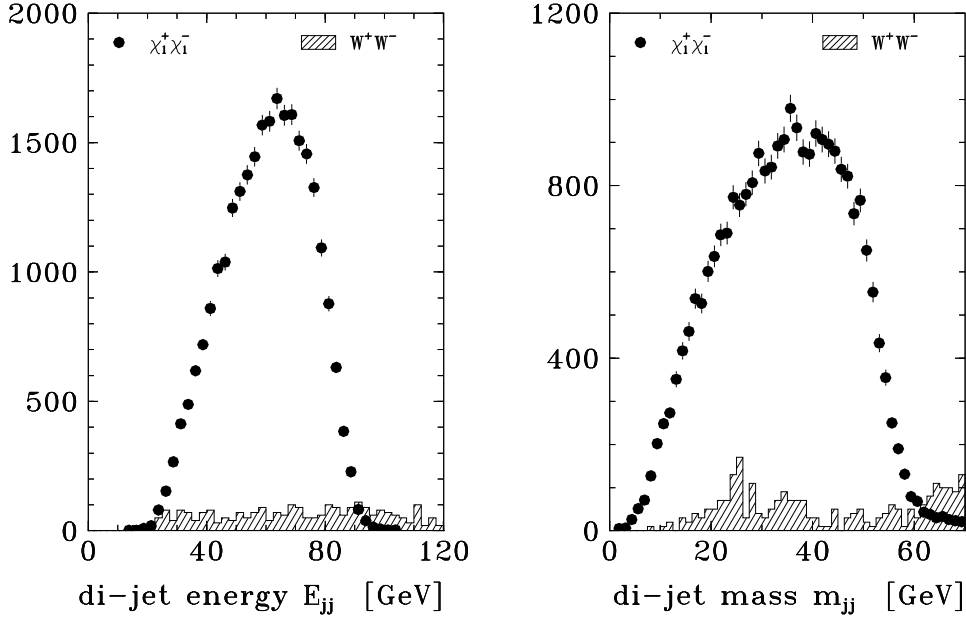


Figure 2.12: Kinematic distributions from a simulation of chargino pair production and decay with 160 fb^{-1} at 320 GeV, from [77]. left: dijet energy distribution; right: dijet mass distribution.

5.2.3 Chargino mass measurement

The process of chargino pair production in e^+e^- annihilation is somewhat more complicated than slepton pair production, but it also provides more interesting observables. To begin, we discuss the chargino mass measurement. If the chargino is the lightest charged supersymmetric particle, it will decay via $\tilde{\chi}_1^+ \rightarrow q\bar{q}\tilde{\chi}_1^0$ or $\tilde{\chi}_1^+ \rightarrow \ell^+\nu\tilde{\chi}_1^0$. The reaction with a hadronic decay on one side and a leptonic decay on the other provides a characteristic sample of events which can be distinguished from W pair production by their large missing energy and momentum. If the lab frame energy of the $q\bar{q}$ system is measured, the kinematic endpoints of this distribution can be used to determine the mass of the $\tilde{\chi}_1^+$ and of the $\tilde{\chi}_1^0$, as in the slepton case. The power of this kinematic fit can be strengthened by segregating events according to the measured value of the $q\bar{q}$ invariant mass. The distributions in the energy and mass of the $q\bar{q}$ system are shown in Fig. 2.12. In the study of [77], one finds mass determinations at the 0.2% level for event samples of the same size as those used in the slepton case.

At large $\tan\beta$ values, the lighter stau ($\tilde{\tau}_1$) may be lighter than the lightest chargino ($\tilde{\chi}_1^\pm$). The decay $\tilde{\chi}_1^\pm \rightarrow \tilde{\tau}_1^\pm\nu_\tau$, followed by $\tilde{\tau}_1^\pm \rightarrow \tilde{\chi}_1^0\tau^\pm$, alters the phenomenology of the chargino production [80]. In this case, one can still measure the mass of a 170 GeV chargino to better than 5 GeV with 200 fb^{-1} at $\sqrt{s} = 400 \text{ GeV}$ [84].

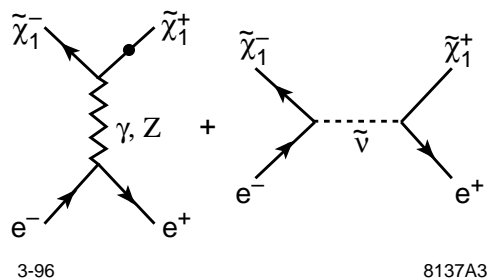


Figure 2.13: Diagrams contributing to chargino pair production.

5.2.4 Analysis of chargino mixing

The cross section and angular distribution of chargino pair production is built up from the diagrams shown in Fig. 2.13. This process is intrinsically more complicated than slepton pair production because one must account for chargino mixing. In supersymmetry models, there is always a charged Higgs boson H^\pm , and both the W^\pm and the H^\pm have spin- $\frac{1}{2}$ partners. These necessarily mix, through a mass matrix of the following form:

$$(\tilde{w}^- \quad i\tilde{h}_1^-)^T \begin{pmatrix} m_2 & \sqrt{2}m_W \sin \beta \\ \sqrt{2}m_W \cos \beta & \mu \end{pmatrix} \begin{pmatrix} \tilde{w}^+ \\ i\tilde{h}_2^+ \end{pmatrix}, \quad (2.15)$$

where \tilde{w}^\pm are the superpartners of the W^\pm and \tilde{h}_1^- and \tilde{h}_2^+ are the superpartners of the charged components of the two Higgs fields. The matrix depends on the parameters μ , the supersymmetric Higgs mass, m_2 ; the supersymmetry breaking mass of the \tilde{w}^\pm ; and $\tan \beta$, the ratio of Higgs field vacuum expectation values. The neutralino masses involve a similar mixing problem among four states, the superpartners of the neutral $SU(2)$ and $U(1)$ gauge bosons and the two neutral Higgs fields. The neutralino mass matrix involves the same three parameters μ , m_2 , $\tan \beta$, plus m_1 , the supersymmetry breaking mass of the \tilde{b} .

Chargino and neutralino mixing is not an added complication that one may introduce into supersymmetric models if one wishes. It is an intrinsic feature of these models which must be resolved experimentally. Unless this can be done, supersymmetry measurements can only be interpreted in the context of model assumptions. In addition, this measurement is important in resolving the question of whether the lightest neutralino in supersymmetry can provide the cosmological dark matter. In most scenarios of the dark matter, the neutralino must be light and dominantly gaugino rather than Higgsino. In any case, the neutralino mixing must be known to build a quantitative theory of the cosmological neutralino production and relic abundance.

Fortunately, it is possible to measure the chargino and neutralino mixing angles by making use of the special handles that the linear collider offers. To see this, consider

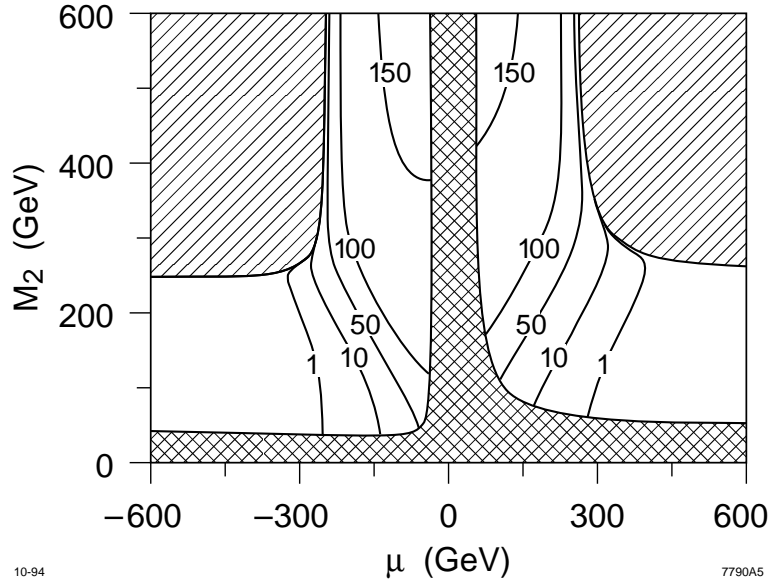


Figure 2.14: Total cross section for $e_R^- e^+ \rightarrow \tilde{\chi}_1^+ \tilde{\chi}_1^-$, in fb, as a function of the chargino mass parameters m_2 and μ .

the diagrams of Fig. 2.13 for a right-handed polarized electron beam. The second diagram, which involves the sneutrino, couples only to left-handed electrons and so vanishes in this case. At high energy, the γ and Z exchanged in the first diagram can be traded for the neutral $SU(2)$ and $U(1)$ gauge bosons. The e_R^- does not couple to the $SU(2)$ boson. The \tilde{w}^\pm does not couple to the $U(1)$ boson. Thus, the total cross section for the process $e_R^- e^+ \rightarrow \tilde{\chi}_1^+ \tilde{\chi}_1^-$ can be large only if the lighter charginos $\tilde{\chi}_1^+$ and $\tilde{\chi}_1^-$ are dominantly composed of the Higgs field superpartners. This remarkable feature is evident in the contour map of this cross section against μ and m_2 shown in Fig. 2.14. A more detailed analysis shows that, by measuring the angular distribution of chargino pair production, one can determine the separate mixing angles for the positive and negative (left-handed) charginos [85]. Unless the mixing angles are very small, the measurement of the two mixing angles and the $\tilde{\chi}_1^+$ mass allow the complete mass matrix (2.15) to be reconstructed. In an example studied in [85], this analysis gave a 10% measurement of $\tan \beta$, purely from supersymmetry measurements, in a 100 fb^{-1} experiment at 500 GeV.

Having determined the chargino mixing, one can then analyze chargino pair production from left-handed fermions. This brings back the dependence on the sneutrino mass. In fact, it is possible to measure the effect of sneutrino exchange and thus to determine the masses of the left-handed sleptons for slepton masses up to a factor of 2 above the collider center of mass energy. Measurements of the ratio of leptonic to hadronic chargino decays also can give information on the masses of the left-handed

sleptons [86]. This can provide a consistency test on the supersymmetry parameters or a target for an energy upgrade.

In both the chargino and slepton studies that we have discussed, it is remarkable how the use of polarization and detailed angular distribution measurements can offer new information along a dimension quite orthogonal to that probed by simple mass determinations. The use of beam polarization is particularly incisive in separating complex composite observables into quantities with a direct relation to the parameters in the underlying Lagrangian.

5.3 Studies of the top quark

The top quark’s special status as the most massive known matter particle, and the only fermion with an unsuppressed coupling to the agents of electroweak symmetry breaking, make it a prime target for all future colliders. The linear collider, operating near the top quark pair-production threshold and at higher energies below 500 GeV, can carry out a complete program of top quark physics. This includes the measurement of the top quark mass, width, form factors, and couplings to many species. This broad program of measurements is reviewed in [87]. In this section, we will discuss two particularly important measurements from this collection.

The mass of the top quark is a fundamental parameter in its own right, and it is also an ingredient in precision electroweak analyses and theories of flavor. It is important to measure this parameter as accurately as possible. Future measurements at the Tevatron and the LHC are likely to determine m_t to 2–3 GeV precision, dominated by systematic effects [88,62].

At the linear collider, the top quark mass is determined directly by the accelerator energy at which one sees the onset of $t\bar{t}$ production. A simulation of the top quark threshold scan, from [89], is shown in Fig. 2.15. Given a measurement of α_s from another source, this scan determines m_t to 200 MeV using only 11 fb^{-1} of data. In the part of the cross section described by the top quark threshold, the t and \bar{t} are separated by a distance small compared to the QCD scale. This means that the mass determined from the threshold scan—as opposed to the ‘pole mass’ determined by the kinematics of high energy production—is a true short-distance quantity which is free of nonperturbative effects. The theoretical error for the conversion of the e^+e^- threshold position to the \overline{MS} top quark mass relevant to grand unified theories is about 300 MeV [90,91]; for the pole mass, it is difficult even to estimate this uncertainty. The expenditure of 100 fb^{-1} at the $t\bar{t}$ threshold allows additional measurements that, for example, determine the top quark width to a few percent precision [92,93,94].

A second important set of measurements is the study of the top quark couplings to γ , Z , W . In the reaction $e^+e^- \rightarrow t\bar{t}$, the final state can be reconstructed as a 6-jet or 4-jet plus $l\nu$ system. The b jets should be identified with an efficiency greater than 80%. Both the production through γ and Z and the decay by $t \rightarrow W^+b$ are maximally parity violating. Thus, there are many independent kinematic variables

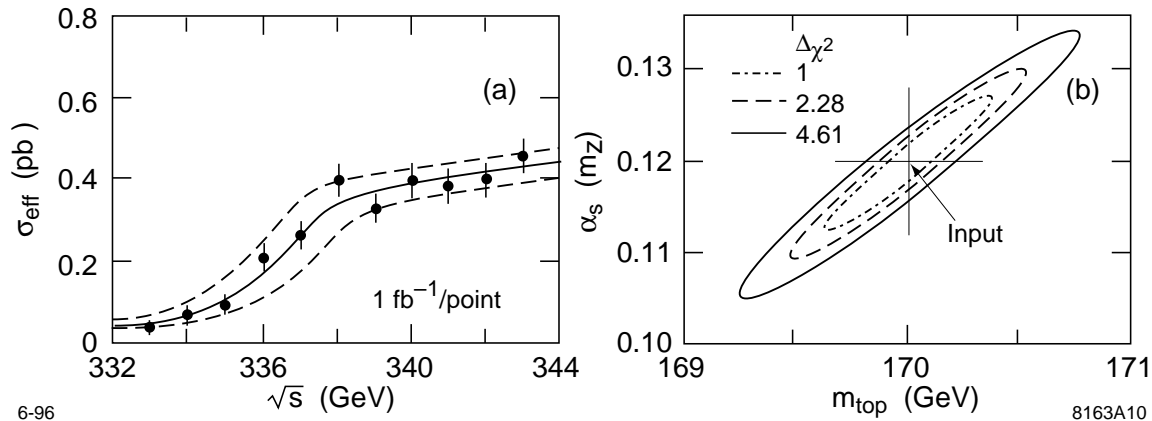


Figure 2.15: Measurement of the top quark mass from the threshold shape, using a threshold scan with a total data sample of 11 fb^{-1} . The effects of beamstrahlung, initial state radiation, and accelerator energy spread are included. A top quark mass of 170 GeV was assumed in this study [89].

that can be used to constrain the various possible production and decay form factors. A simulation study using 80% e^- beam polarization but only 10 fb^{-1} of luminosity at 500 GeV showed that it is possible to simultaneously constrain the whole set of vector and axial vector γ , Z , and W form factors of the top quark with errors in the range $5\text{--}10\%$ [87]. This analysis should improve further with high-luminosity data samples [95]. Experiments at the linear collider are sensitive at similar levels to anomalous couplings of $t\bar{t}$ to the gluon [96].

A set of couplings of particular interest are the vector and axial $t\bar{t}Z$ form factors. As we have explained in Section 4.5, these form factors are predicted to receive large contributions in certain models of strong-interaction electroweak symmetry breaking. These contributions result from diagrams in which the Z couples to the new strongly-interacting species which break electroweak symmetry, and these couple to the top quark through the mechanism which generates the top quark mass [28]. In Fig. 2.16, the Z form factor determinations from the simulation study of [97] are compared to two representative theories [1]. It is interesting that most of the sensitivity in this particular measurement comes from the polarization asymmetry of the total top pair production cross section. The measurement of this quantity is dominated by statistics and can be improved straightforwardly with higher luminosity.

An additional important measurement is the determination of the top quark Higgs Yukawa coupling. At the LHC, the ratio $\lambda_{t\bar{t}h}/\lambda_{WW_h}$ can be measured to an accuracy of 25% for $80 < m_h < 120 \text{ GeV}$ [62]. At a linear collider, the top quark Yukawa coupling can be measured by studying the process $e^+e^- \rightarrow t\bar{t}h^0$, relying on the $b\bar{b}$ decay of the h^0 to produce spectacular events with 4 b 's in the final state. This process is difficult to study at 500 GeV , but it becomes tractable at higher energy. In

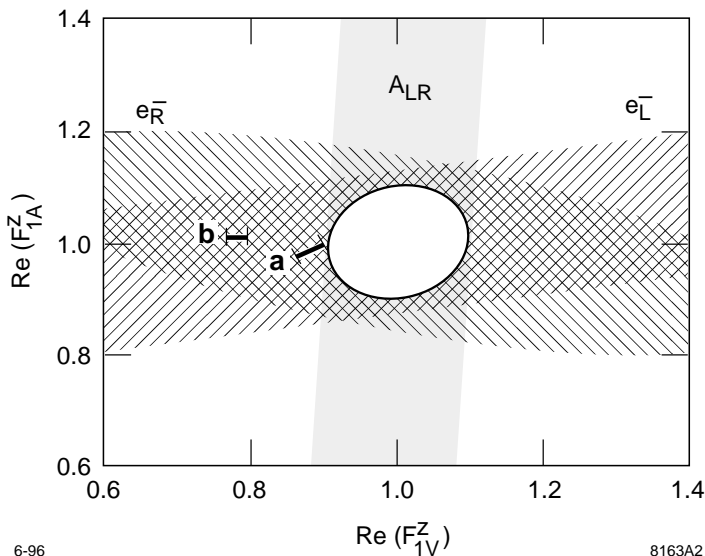


Figure 2.16: Determination of the form factors for the vector and axial vector couplings of the top quark to the Z , with 100 fb^{-1} at 400 GeV [97], compared to the predictions of technicolor models, from [1].

simulation studies at 800 GeV , where the cross section is about 8 times higher than at 500 GeV , a 1000 fb^{-1} sample yields a 6% uncertainty on $\lambda_{t\bar{t}h}$ for a 120 GeV Higgs boson [98,99].

5.4 Studies of W boson couplings

Recent experiments at LEP 2 and the Tevatron have observed weak boson pair production and have verified the general expectations for the cross sections given by the Standard Model [100,101]. This is already an important discovery. One of the motivations for building a model of the weak-interaction bosons from a Yang-Mills gauge theory is that the special properties of the Yang-Mills coupling tame the typically bad high energy behavior of massive vector fields. We now know that the behavior of the W and Z production cross sections, at least in the region close to threshold, conforms to the gauge theory predictions.

This discovery sets the stage for the use of W and Z bosons to probe the physics of electroweak symmetry breaking. As we have noted in Section 4.5, new strong interactions that might be responsible for electroweak symmetry breaking can affect the three- and four-particle couplings of the weak vector bosons. The precision measurement of these effects—and the corresponding effects on the top quark couplings discussed in the previous section—can provide a window into the dynamics of electroweak symmetry breaking complementary to that from direct W boson scattering.

Our discussion in Section 4.5 implies that a high level of precision is necessary. We

estimated there that effects of new strong interactions affect the standard parameters used to describe the $WW\gamma$ and WWZ vertices— κ_V , λ_V , for $V = \gamma, Z$, and g_Z —at the level of a few parts in 10^{-3} . For comparison, the one-loop radiative corrections to these parameters predicted in the Standard Model are of the order of 10^{-3} – 10^{-4} [102].

In contrast, the current bounds on parameters of the W vertices from LEP 2 and the Tevatron are at the level of 10^{-1} [100,101,103]. Much improved constraints are expected from the LHC. There one expects to place bounds on the WWV couplings in the range [62,104]

$$|\Delta\kappa_V| < 0.01 \text{ to } 0.1, \quad \left| \Delta g_1^Z \right|, \quad |\lambda_V| < 0.001 \text{ to } 0.01 \quad (2.16)$$

which might be sensitive to effects of new physics. It should be noted that the LHC analyses integrate over a large range of center-of-mass energies for vector boson pair production. This means that the sensitivity and interpretation of these experiments depend on assumptions about the energy-dependence of the form factors describing the new physics effects.

The linear collider provides an ideal laboratory for the study of the WWV couplings. The process $e^+e^- \rightarrow W^+W^-$ actually gives the largest single contribution to the e^+e^- annihilation cross section at high energies. The W pair events can be reconstructed in the four-jet final state. More importantly, the events with a leptonic decay on one side and a hadronic decay on the other allow unambiguous reconstruction of the charge and decay angles of the leptonic W . Both the production process and the W decay are strongly parity-violating, so both beam polarization and angular distributions can be used to extract the details of the W vertices. The diagrams for $e^+e^- \rightarrow W^+W^-$ involve both γ and Z , but these effects can be disentangled by the use of beam polarization. The W pair production cross section is about 30 times larger with left-handed than right-handed polarized beams. The suppression of the right-handed cross section depends on the relation between the $WW\gamma$ and WWZ vertices predicted by the Standard Model and so is a sensitive measure of deviations from this prediction.

Effects from strong-interaction electroweak symmetry breaking, which enter through effective Lagrangian parameters as in (2.9), affect the cross section for longitudinal W pair production through terms proportional to (s/m_W^2) . At the same time, the fraction of the cross section with longitudinal W pairs grows as $\beta^2 = (1 - 4m_W^2/s)$. From these two effects alone, one should expect a factor 15 improvement in the sensitivity to these effects in going from LEP 2 to the linear collider experiments at 500 GeV. The most important advantage, however, is the increase in statistics with high luminosity running. A recent simulation of the WWV coupling measurement at a 500 GeV collider with 500 fb^{-1} estimates the limits that can be placed on the coupling parameters as [105]

$$\left| \Delta g_1^Z \right| < 2.5 \times 10^{-3}, \quad |\Delta\kappa_Z| < 7.9 \times 10^{-4}, \quad |\lambda_Z| < 6.5 \times 10^{-4}, \quad (2.17)$$

$$|\Delta\kappa_\gamma| < 4.8 \times 10^{-4}, \quad |\lambda_\gamma| < 7.2 \times 10^{-4}. \quad (2.18)$$

These results qualitatively improve on the LHC sensitivity, to the point where not only effects of new physics but even the Standard Model radiative corrections are visible.

5.5 Studies of QCD

In addition to the search for new physics, the linear collider will be able to complete the program of precision tests of the Standard Model with a precise measurement of the QCD coupling constant α_s . The strong coupling constant is determined in e^+e^- annihilation from the production rate for 3-jet events. The reduction in the relative size of hadronization effects at high energy allow a measurement of α_s with systematic errors smaller than 1% [106].

A measurement of α_s of similar quality can be obtained from the ratio of hadronic to leptonic decays of the Z^0 , if one can obtain a sample of more than 10^8 Z^0 decays. This becomes practical in linear collider experiments at the Z^0 , as we will explain in Section 5.6. By comparing the two precision measurements of α_s at Q values of m_Z and 500 GeV, it will be possible to give a precise test of the QCD renormalization group equation.

With confidence in the running of α_s from this experiment, one can extrapolate the precise value of α_s to the grand unification scale. Current data is consistent with a grand unification with the renormalization group equations of supersymmetry; however, it gives little constraint on the details of unification. With an accurate α_s , one can anticipate a precise test of grand unification relations. The contributions to be accounted for include next-to-leading order corrections from two-loop beta functions, TeV-scale threshold effects, and GUT-scale threshold effects [36]. The two-loop beta functions are known from the general theoretical scheme. The TeV-scale threshold effects are unknown today, but they will be determined from the new particle masses measured at the LHC and the linear collider. Then a 1% measurement of α_s would allow a 10% measurement of the GUT-scale threshold correction. This measurement would give an indirect but significant constraint on the spectrum of the massive particles responsible for the GUT level of fundamental symmetry breaking.

The linear collider can also provide the most sensitive experiments on photon structure, including the precise measurement of the photon structure function F_2^γ . In addition, with sufficient forward instrumentation, the linear collider could study $\gamma^*\gamma^*$ scattering at large s and fixed momentum transfer. This is a beautifully clean model system for analyzing a part of QCD that is still very mysterious, the nature of the pomeron and the dynamics of high-energy scattering [107].

Parameter	Current Value	LC Measurement
$\sin^2 \theta_W^{\text{eff}}$	0.23119 ± 0.00021	± 0.00002
m_W	$80.419 \pm 0.038 \text{ GeV}$	$\pm 0.006 \text{ GeV}$
$\Gamma(Z \rightarrow \ell^+ \ell^-)$	$83.96 \pm 0.09 \text{ MeV}$	$\pm 0.04 \text{ MeV}$
$R_b^{\text{exp}}/R_b^{\text{th}}$	1.0029 ± 0.0035	± 0.0007
$A_b^{\text{exp}}/A_b^{\text{th}}$	0.958 ± 0.017	± 0.001

Table 2.4: Current values of some important electroweak parameters, and the potential uncertainty obtainable at a linear collider providing with high statistics (*e.g.*, $10^9 Z^0$ decays).

5.6 Precision electroweak studies

In addition to the experimental program at 500 GeV energies, one can envision using the linear collider at the Z^0 and the W threshold to carry the experimental program of precision electroweak measurements to the next level. Operation of the linear collider at the Z^0 pole would yield more than $10^9 Z^0$ decays in a 20 fb^{-1} data sample. With more than 100 times LEP 1 statistics and high beam polarization, one could undertake a very ambitious and extensive program of precision measurements. For example [108], employing the left-right polarization asymmetry, leptonic forward-backward asymmetries, and tau polarization asymmetry (all of which are currently statistics limited) one could improve the determination of $\sin^2 \theta_W^{\text{eff}}$ at the Z pole by an order of magnitude, bringing it to an unprecedented $\pm 0.01\%$ level. Other quantities such as the Z line shape parameters, $R_b = \Gamma(Z \rightarrow b\bar{b})/\Gamma(Z \rightarrow \text{hadrons})$, and A_b (the polarized $b\bar{b}$ asymmetry) could also be improved. They would be limited only by systematics.

With such a large sample of Z decays, one would have more than $10^8 b\bar{b}$ and $3 \times 10^7 \tau^+ \tau^-$ pairs. The study of these events could make use of the outstanding vertex resolution and detection efficiency of the linear collider environment. In addition, polarized $e^+ e^-$ annihilation at the Z^0 produces (for a left-handed beam) dominantly forward production of b quarks and backward production of antiquarks, thus eliminating the need for a flavor tag. These features combine to give an ideal environment for studying CP violating asymmetries and rare decays as well as performing precision measurements [108]. For example, one could improve the current precision on the forward-backward asymmetry parameter A_b by more than an order of magnitude.

In Table 2.4, we have listed some improved measurements envisioned at the linear collider. The tiny error on $\sin^2 \theta_W^{\text{eff}}$ assumes a precise beam polarization measurement that may require polarizing both the electron and positron beams. The importance of refining $\sin^2 \theta_W^{\text{eff}}$ is well illustrated by the prediction for the Higgs mass that would be obtained by employing these precise values and the improved value of m_t from

Section 5.4 as input. One finds

$$m_h = (140 \pm 5 \text{ GeV})e^{[1911(\sin^2 \theta_W^{\text{eff}} - 0.23158)]}, \quad (2.19)$$

where the dominant error comes from hadronic loop uncertainties in α (assumed here to be reduced by a factor of 3 compared to the current error). Comparison of the indirect loop determination of m_h from (2.19) with the direct measurement of m_h from the LHC and the linear collider would confront the electroweak prediction at the 5% level and would provide an accurate sum rule to be satisfied by new heavy particles with electroweak charge. Another way to look at this comparison is that it will probe the S and T parameters to an accuracy of 0.02, about 8 times better than current constraints. At that level, even the existence of a single heavy chiral fermion doublet (much less an entire dynamical symmetry breaking scenario) would manifest itself. The accurate value of $\sin^2 \theta_W^{\text{eff}}$ at the Z pole would be a valuable input to the measurements of cross sections and asymmetries at high energy that we will discuss in Sections 6.3 and 6.4, measurements which probe for possible Z' bosons, lepton compositeness, or new space dimensions.

A linear collider run near the W^+W^- threshold would also be extremely valuable for improving the determination of m_W beyond the capabilities of the LHC [108]. Already at the current uncertainty of 40 MeV, the determination of the m_W mass from kinematic fitting of W pair production at LEP 2 is affected by systematic uncertainty from the modeling of fragmentation. But the interpretation of the measurement of the W threshold position is almost free of theoretical uncertainty, allowing a 6 MeV measurement to be done with a dedicated 100 fb⁻¹ run.

Collectively, the broad program of precision electroweak studies which the high luminosity of the linear collider makes available nicely complements and expands the physics goals at the maximum collider energy.

6 Further topics from the linear collider physics program

In the preceding section, we have discussed only those aspects of the linear collider experimental program for which there are strong arguments that the phenomena to be studied will appear at 500 GeV. There are many other experiments that can be done at an e^+e^- linear collider which has sufficient energy to reach the required threshold for new particles. In this section, we will describe a number of experiments of this character. All of these experiments will eventually become relevant as components of the long-term program that we have described in Section 2. Measurements at the LHC which estimate the new thresholds could provide specific motivation for upgrading a 500 GeV collider to higher energy. But, one should keep in mind that all of the phenomena we describe in this section could well be present at 500 GeV and provide additional richness to the initial physics program of the linear collider.

It is well appreciated that an e^+e^- collider provides an excellent environment to search for all varieties of exotic particles with nonzero electroweak quantum numbers. The huge variety of particles which have been searched for at LEP is described, for example, in [109]. In almost all cases, the LEP limits are close to the kinematic limit allowed by the collider. A collider operating above the pair production threshold will be able to accumulate a large sample of events (70,000 events per unit of R in a 200 fb^{-1} sample at 500 GeV) and make incisive measurements.

The corresponding discovery reach for exotic particles at the LHC ranges from a few hundred GeV for new leptons to about 2 TeV for new quarks. So, as a general statement, the locations of the new thresholds are likely to be found at the LHC. Experimenters at a linear collider will measure essential information that is beyond the capability of the LHC. We have seen examples of this in Section 5, and further examples will be discussed in this section.

Rather than summarize all possible measurements of new phenomena at a linear collider, we restrict ourselves in this section to four specific examples that have been worked out in some detail. In Section 6.1, we will discuss the particles of an extended Higgs sector such as that in the Minimal Supersymmetric Standard Model. In Section 6.2, we will discuss studies of supersymmetric particles beyond the lightest chargino, neutralinos, and sleptons. In Section 6.3, we will discuss new and exotic Z' bosons. In Section 6.4, we will discuss probes of large extra dimensions and TeV-scale quantum gravity.

Because this paper focuses on the issue of a 500 GeV collider, we do not discuss here the significant capabilities of higher energy e^+e^- collisions to probe WW scattering processes [110]. These include the unique ability to study the reaction $W^+W^- \rightarrow t\bar{t}$, which directly tests the coupling of the top quark to the particles responsible for strong-interaction electroweak symmetry breaking. These experiments, and the comparison to the LHC capabilities, are reviewed in [15,111].

Although the detailed physics justification for increased e^+e^- collision energy is more difficult to quantify at present than that for the initial 500 GeV step, we fully expect that the experimentation at the LHC and first stage e^+e^- linear collider will reveal phenomena that dictate energy upgrades. It is important to continue the R&D needed for this evolution.

6.1 Extended Higgs sector

In Section 5.1, we have discussed the measurement of the properties of the lightest Higgs boson. Many models of new physics allow multiple Higgs fields, leading to additional heavier Higgs particles. In particular, supersymmetry requires the presence of at least two Higgs doublet fields. This produces, in addition to the h^0 , four additional states—the CP-even H^0 , the CP-odd A^0 , and charged states H^\pm . The masses of these states should be comparable to the masses of other supersymmetric particles. If the scale of superparticle masses is much greater than 100 GeV, then typically the

four heavy Higgs states are relatively close in mass, and the light h^0 resembles the Higgs boson of the Standard Model.

The heavy Higgs states are very difficult to find at the LHC. The LHC experiments have studied extensively their sensitivity to the Higgs sector of the MSSM. We have already presented a summary of these analyses in Fig. 2.2. A low mass H^\pm can be found at the LHC below about 125 GeV in the decays of the top quark. For m_{H^\pm} above 225 GeV, its decay into $t\bar{b}$ can be used to find the charged Higgs if $\tan\beta \gtrsim 25$ or $\tan\beta \lesssim 2$. In the region of intermediate $\tan\beta$ above the LEP limits, only the process $h^0 \rightarrow \gamma\gamma$ is visible, and the H and A are not seen at all. For larger $\tan\beta$ (> 10), the decays $H/A \rightarrow \tau^+\tau^-$ become accessible. Because the technique for detecting H and A involves particles that decay with missing energy, it will be difficult to make a precise mass measurement. ATLAS studies suggest an accuracy on the H/A mass of about 5 GeV, for $M_{H/A} = 300$ GeV and $\tan\beta = 10$, only after 300 fb^{-1} has been collected. For comparison, the H - A mass difference is at most a few GeV. For low $\tan\beta$, H could be detected by $H \rightarrow ZZ^*$. This mode, however, applies only to a limited region of parameter space, $\tan\beta < 3$ (a region disfavored by the LEP constraint on the mass of h) and $m_H < 350$ GeV.

A crucial aspect of the experimental study of the heavy Higgs states would be to measure the value of $\tan\beta = \langle\phi_2\rangle / \langle\phi_1\rangle$, where ϕ_1 and ϕ_2 are the two Higgs doublets of the MSSM. This quantity is needed to determine the absolute size of the quark and lepton Yukawa couplings. For example, it is possible that the bottom quark Yukawa coupling is large and the lightness of the bottom quark is explained by the fact that the Higgs field responsible for this mass has a small vacuum expectation value. In supersymmetry, $\tan\beta$ also appears in many formulae for the supersymmetry masses and mixings and is a source of theoretical uncertainty unless it can be pinned down. The LHC can measure $\tan\beta$ from the heavy Higgs particles only where H is visible by one of the techniques just listed, to an accuracy of 10–30%. It should be noted that what is measured is $\sigma \cdot BR$, and so the determination of $\tan\beta$ depends on theoretical assumptions about the total width.

If the masses of H , A are well above that of h , these particles are mainly produced at an e^+e^- collider in pairs, through $e^+e^- \rightarrow H^0A^0$. The mass determination is straightforward. Kinematic fitting of decays with $b\bar{b}$ on both sides should give an accuracy of 0.3%. The program described earlier for the precision determination of the h branching fractions can be applied also to the H and A . The crucial parameter $\tan\beta$ is given by the ratio of the branching ratios to $b\bar{b}$ and $t\bar{t}$. For A ,

$$\frac{\Gamma(A \rightarrow t\bar{t})}{\Gamma(A \rightarrow b\bar{b})} = \frac{m_t^2}{m_b^2} \cot^4\beta \cdot \left(1 - \frac{4m_t^2}{m_A^2}\right)^{1/2}. \quad (2.20)$$

From this measurement, a completely model-independent determination of $\tan\beta$ to 10% accuracy is expected. Measurements of other branching fractions of H , A , and H^\pm will provide cross-checks of this value [112].

The ATLAS [62] and CMS [75] analyses of the fitting of LHC data to the minimal supergravity-mediated model gives a remarkable accuracy of 3% in the determination of $\tan\beta$. However, this determination of $\tan\beta$ is based on the assumption of a specific model of supersymmetry breaking. It uses the precision measurement of the h^0 mass and thus depends on the detailed theory of the one-loop supersymmetry corrections to this parameter. Linear collider experiments offer a number of methods to determine $\tan\beta$ from supersymmetry observables in a model-independent way. For example, $\tan\beta$ can be extracted from chargino mixing, as we have discussed in Section 5.2.4. In the end, it is a nontrivial test of the theory whether the determinations of $\tan\beta$ from the supersymmetry spectrum agree with the direct determination of this parameter from the Higgs sector.

6.2 Supersymmetric particle studies

In Section 4.4, we have argued that, if the new physics at the TeV scale includes supersymmetry, the lightest supersymmetric particles are likely to appear at a 500 GeV e^+e^- collider. In Section 5.2, we have discussed the program of detailed measurements on those particles. Of course, nothing precludes a larger set of supersymmetric particles from appearing at 500 GeV, though it is likely that increased energy will be needed to produce the full supersymmetry spectrum. In this section, we will discuss what can be learned from a more complete study of the supersymmetry spectrum in e^+e^- annihilation.

For brevity, we focus on two important issues. The first of these is whether supersymmetry does in fact give the dynamics that leads to electroweak symmetry breaking. To verify the mechanism of electroweak symmetry breaking experimentally, we must determine the basic parameters that directly determine the Higgs potential. These include the heavy Higgs boson masses discussed in the previous section. Another essential parameter is μ , the supersymmetric Higgs mass parameter. As we have discussed in Section 5.2, this parameter can already be determined from the study of the lighter chargino if these particles are not almost pure \tilde{w} . In that last case, μ is determined by measuring the mass of the heavier charginos. We have argued in Section 4.4 that these particles should be found with at most a modest step in energy above 500 GeV. A precision mass measurement can be done using the endpoint technique discussed in Section 5.2.

In typical supersymmetric models, the negative Higgs (mass)² which causes electroweak symmetry breaking is due to a mass renormalization involving the top squarks. This same renormalization leads to \tilde{t}_L - \tilde{t}_R mixing and to a downward shift in the top squark masses relative to the masses of the first- and second-generation squarks. The mass shift, at least, might be measured at the LHC. However, in some scenarios with a large mass shift, only the third-generation squark masses can be measured accurately [62]. At the linear collider, flavor-dependent squark masses can be measured to accuracies better than 1%. In addition, the mass differences of the partners of q_L

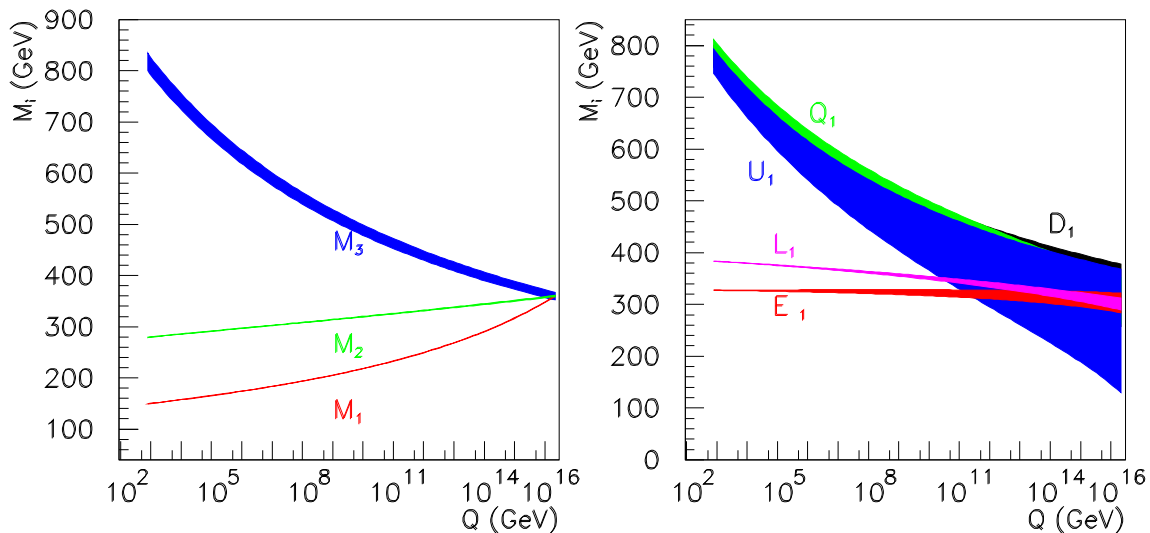


Figure 2.17: Extrapolation of supersymmetry mass parameters determined at a linear collider from the TeV scale to the grand unification scale, from [115]. The width of each band at the weak scale is the error in the direct parameter determination; these errors are propagated to higher energies using the renormalization group equations.

and q_R can be measured to this accuracy using polarization asymmetries [113]. By comparing the pair production cross sections with polarized beams, as described in Section 5.2 for stau mixing, it is possible to measure the top squark mixing angle to better than 1% accuracy in a 500 fb^{-1} experiment [114].

The second issue is the possibility of the grand unification of supersymmetry breaking parameters. This is the crucial test of whether supersymmetry breaking arises from physics above the grand unification scale or from a different mechanism acting at lower energies. This test requires accurate model-independent determinations of as many supersymmetry mass parameters as possible. Figure 2.17 shows an extrapolation to the grand unification scale at $2 \times 10^{16} \text{ GeV}$ of masses determined in a 500 fb^{-1} sample at a linear collider. The most effective tests of grand unification come from the comparison of the gaugino mass parameters m_1 and m_2 and from comparison of the masses of the sleptons \tilde{e}_R and \tilde{e}_L (called E_1 and L_1 in the figure). Because of QCD threshold corrections, the masses of the gluino (m_3) and the first-generation squarks (labeled D_1 , Q_1 , U_1) are less effective in this comparison. It should be noted that the mass ratios which provide the most significant tests of grand unification are just the ones that are most difficult to measure accurately at the LHC. Even for the uncolored states, a 1% mass error at the weak scale evolves to a 10% uncertainty at the grand unification scale. So this comparison puts a premium on very precise mass determinations, such as a linear collider will make possible.

These issues are only two slices through the rich phenomenology of supersymmetric

particles. If supersymmetric particles—or any other family of exotic particles—appear at the TeV scale, there will be a full program of experiments for both hadron and e^+e^- colliders.

6.3 New Z' bosons

The new physics at the TeV scale must have $SU(3) \times SU(2) \times U(1)$ gauge symmetry, but it might have an even larger gauge symmetry with additional heavy vector particles. The simplest extensions are those with extra $U(1)$ gauge symmetries. The corresponding gauge bosons appear as new vector resonances— Z' bosons—coupling to lepton and to $q\bar{q}$ pairs.

Extra $U(1)$ factors in the gauge group preserve the predictions of grand unification. In fact, these new symmetries appear naturally in models in which the grand unification group is larger than the minimal choice of $SU(5)$. For example, the grand unification group E_6 contains the Standard Model gauge group and two additional $U(1)$ factors. This leads to models in which the gauge symmetry at TeV energies contains an additional $U(1)$ factor which is a linear combination of these [116,117].

In certain grand unified models, the masses of the heavy neutral leptons which give the scale of the neutrino mass seesaw are determined by the scale of breaking of an extra $U(1)$ symmetry. In this case, the extreme lightness of neutrinos puts the mass of the Z' beyond the reach of accelerator experiments. But many other motivations for a new $U(1)$ symmetry point to lower masses [118]. In particular, the size of the μ parameter of supersymmetry may be controlled by the scale of breaking of a $U(1)$ symmetry, in which case the corresponding Z' boson must have a mass not far above 1 TeV. More generally, the possible richness of gauge symmetries motivates the search for these new states. This is especially true for superstring theories, where explicit model constructions often predict a large number of extra $U(1)$ gauge particles [119].

The abilities of colliders to detect signatures of heavy Z' bosons have been studied in great detail. Hadron colliders have impressive sensitivity for searches in which the Z' bosons appear as resonances decaying to $\ell^+\ell^-$. Lepton colliders can be sensitive to Z' bosons in a different way, through the precision study of the pair production processes $e^+e^- \rightarrow \ell^+\ell^-$ and $e^+e^- \rightarrow q\bar{q}$. Because these reactions can be measured precisely and also predicted theoretically to part per mil accuracy, experiments can be sensitive to interference effects caused by Z' bosons of mass a factor of 10 or more above the e^+e^- center of mass energy [120,121,122]. All of the special handles of the e^+e^- environment, including polarization asymmetries, flavor tagging, and τ polarization, can be brought to bear in the search for these interference effects.

Table 5, based on [123], gives a comparison between the sensitivity of e^+e^- linear colliders and that of the LHC. The models listed in the table correspond to particular choices for the quantum number assignments of the Z' ; see the original reference for details. The table shows that the sensitivity of a linear collider operating at 500 GeV is quite comparable to that of the LHC. The sensitivities quoted in the table correspond

Model	500 GeV	1000 GeV	LHC
χ	4.5	6.5	4.5
ψ	2.6	3.8	4.1
η	3.3	4.7	4.2
I	4.5	6.5	4.4
SSM	5.6	8.1	4.9
ALRM	5.4	7.9	5.2
LRM	5.2	7.5	4.5
UUM	6.7	9.8	4.6

Table 2.5: Sensitivity of e^+e^- linear colliders and the LHC to effects of a Z' , after [123]. The table gives the mass reach in TeV for observability at the 95% CL. The analysis for linear colliders is based on measurement of indirect effects for an event sample of 200 fb^{-1} ; it includes the effect of experimental cuts. The analysis for the LHC gives the direct sensitivity to a resonance, assuming an event sample of 100 fb^{-1} and Z' decays only to Standard Model fermions.

to different types of measurements, and this point illustrates the complementary relation of the LHC and the linear collider. For a Z' at a few TeV, the LHC will identify a resonance and accurately measure the mass M . The linear collider will measure interference effects and thus determine the quantity $g_e g_f / M^2$ which depends on the mass and the coupling strengths to the electron and the flavor f . By combining these pieces of information, one may obtain a complete phenomenological profile of the Z' . Both hadron and lepton collider experiments will thus be needed to understand how the Z' fits into the larger picture of unification and symmetry.

This study of $e^+e^- \rightarrow f\bar{f}$ can also be used to search for composite structure of quarks and leptons. The process most sensitive to compositeness is Bhabha scattering. A 200 fb^{-1} experiment at 500 GeV would be expected to place a limit of 90 TeV on the Λ parameters of electron compositeness. Møller scattering ($e^-e^- \rightarrow e^-e^-$) potentially provides an even more sensitive probe, offering a limit of 130 TeV for a 200 fb^{-1} experiment at 500 GeV [124]. Even the e^+e^- limit is a factor of 6 above the expected limit from studies of Drell-Yan production at the LHC [62]. In addition, an effect seen at the LHC could come from any one of a large number of possible operators, while in polarized Bhabha or Møller scattering the operator structure can be determined uniquely.

6.4 Large extra dimensions

Among the most remarkable proposals for new physics at the TeV scale is the idea that new space dimensions play an important role. String theorists have insisted

for many years that Nature contains more than four dimensions. However, for a long time the extra dimensions were considered to be unobservably small. Recently, new developments in string theory and phenomenology have shaken up this complacent picture and have suggested that new space dimensions may be of the size \hbar/TeV , or even larger [125,126,127].

There is no space here for a complete review of these new developments. (A brief review can be found in [128].) But we would like to indicate the role that the LHC and the linear collider could play in the elucidation of these models.

Consider first models in which there is a single new dimension of TeV size. In this model, the basic quantum fields in Nature are five-dimensional. The momentum in the fifth dimension is quantized and can be interpreted as the mass of a four-dimensional field. So, each quantized value of the fifth component of momentum gives a state that we would observe as a new heavy particle. The easiest states to observe are the components of the photon and Z with nonzero momentum in the fifth dimension. These would appear as Z' bosons. The sensitivity of the LHC and the linear collider to these states is greater than that to the ‘SSM’ (Sequential Standard Model) boson listed in Table 5. If several states can be discovered, one can begin to map out the geometry of the extra dimensions. A similar phenomenology applies to the Randall-Sundrum model [129] in which curvature in the fifth dimension is used to explain the hierarchy between the Planck scale and the weak scale. In this case, the new resonances are actually higher Fourier components of the gravitational field, a fact which can be recognized experimentally by their characteristic spin-2 decay distributions [130].

In another class of models, our apparently four-dimensional world is a membrane in a space of larger dimensionality [127]. This scheme allows the scale at which quantum gravity becomes a strong interaction to be much lower than the apparent Planck scale. In fact, it can be as low as TeV energies. The authors of [127] emphasized that their theory could be tested by macroscopic gravity experiments. But in fact more stringent tests come from high energy physics, from experiments that look for the effects of gravitational radiation at high energy colliders. These are of two types. First, if the scale M of strong quantum gravity is low, one expects radiation of gravitons G in e^+e^- and $q\bar{q}$ collisions, giving rise to processes such as

$$e^+e^- \rightarrow \gamma G \quad q\bar{q} \rightarrow gG \quad (2.21)$$

which appear as photons or jets recoiling against an unobserved particle. These effects have been searched for explicitly at LEP and the Tevatron (*e.g.*, [131]), giving lower limits of about 1 TeV on the gravity scale M . Second, one can look for the effects of virtual graviton exchange interfering with Standard Model annihilation processes. These interference effects have been searched for both by measurements of e^+e^- annihilation to fermion pairs at LEP 2 (*e.g.*, [132]) and by measurements of Drell-Yan

and $\gamma\gamma$ pair production at the Tevatron [133]. In both cases, the sensitivity to M reaches above 1 TeV.

These experiments will be repeated at the next generation of colliders. The limits on M from missing energy experiments are expected to be about 5 TeV from the high luminosity linear collider at 500 GeV, and about 8 TeV from monojet searches at the LHC. Similarly, limits on M from virtual graviton exchange should reach to about 6 TeV both at the 500 GeV linear collider and in the study of Drell-Yan processes at the LHC [134]. These values are high enough that, if the new dimensions are actually connected to the physics of the TeV scale, their effects should be observed. In that case, the linear collider experiments will take on an added significance. At the linear collider, but not at the LHC, it is possible to determine the parton kinematics of a missing energy event. Then one can determine whether events have a broad mass spectrum, as predicted in ordinary quantum gravity, or whether they are resonant at fixed mass values, as predicted in string theory. For virtual graviton processes, the linear collider can observe the flavor- and helicity-dependence of the interference effects and determine whether the new couplings are universal, as naively expected for gravity, or are more complex in nature.

If there are more than four dimensions in Nature, the evidence for this will most likely come from high-energy physics. The possibility provides a tremendous opportunity, one which will engage experimenters at both hadron and lepton colliders.

7 Conclusions

The beautiful experiments in particle physics over the past 20 years and the tremendous theoretical effort to synthesize the current understanding of electroweak symmetry breaking have brought us to a point of exceptional opportunity for uncovering new laws of physics. The wealth of precision electroweak measurements indicate that a new threshold is close at hand. The precision measurements place strong constraints on models that explain the symmetry breaking and point to new phenomena at the 500 GeV scale.

Later in this decade, we will begin to capitalize on this opportunity with experiments at the LHC. There is no doubt that the LHC will make important discoveries. However, many crucial measurements on the expected new physics are difficult to perform at a hadron collider. In this paper we have argued that a 500 GeV linear collider will provide essential information needed to interpret and to exploit these discoveries.

The LHC should discover a Higgs boson (if LEP 2 or Tevatron experiments have not already done so) in all but rather special circumstances. The linear collider is very well suited to measuring its quantum numbers, total width and couplings. Moreover, if there is an expanded Higgs sector, measurement of the Higgs couplings to fermion

pairs and to gauge bosons is essential.

If the new physics includes supersymmetry, the LHC experiments should observe supersymmetric particle production. They will measure some fraction of the sparticle masses, but they most likely will not be able to determine their spin and electroweak quantum numbers. Measurement of mixing angles and supersymmetric couplings at the LHC will be very difficult. To the extent that the sparticles are accessible to a linear collider, these measurements are straightforward and precise. We have argued that there is a good probability that some of the crucial sparticles will be within reach of a 500 GeV collider. The measurements of gaugino and sfermion mixings and masses will provide important clues towards understanding how supersymmetry is broken and transmitted to the TeV scale.

We have reviewed the models in which new strong interactions provide the means by which the Standard Model particles acquire mass, and have found that although such models cannot be ruled out, they have become increasingly constrained by the existing precision data. The LHC has the possibility for observing new strong interactions through modifications to WW scattering. We have argued that analogous modifications to the gauge boson or top quark couplings can be seen with a 500 GeV linear collider. We have also suggested that operation of the linear collider at the Z resonance may be profitable.

In each of these examples, we have argued that the linear collider and the LHC have complementary roles to play. It is likely that neither machine, by itself, will piece together the full picture of electroweak symmetry breaking. The strength of the LHC is its large partonic energy and copious production of many new particles. The linear collider, with its control of partonic energy and beam polarization, and with favorable signal to background ratios, can make crucial measurements that reveal the character of new phenomena. The complementarity of hadron and lepton collisions has been amply demonstrated in the past, and there is every reason to expect that it will continue in the future.

It may be useful to give a few illustrative examples of how the linear collider program might respond to possible outcomes of the LHC experiments:

1. *A Higgs-like state is discovered below 150 GeV, and strong evidence for supersymmetry is found.* In this case, the linear collider program would be based primarily on the exploration of supersymmetry and the extended Higgs sector. It would measure the couplings, quantum numbers, mixing angles and CP properties of the new states. These precisely measured parameters hold the key for understanding the mechanism of supersymmetry breaking. In this scenario, a premium would be placed on running at sufficiently high energy that the sparticles are produced. This might dictate raising the energy to at least 1 TeV.
2. *A Higgs particle is seen, and no evidence for supersymmetry is found.* The key

objective in this scenario would be the thorough investigation of the Higgs particle. Here, precision measurements would be of paramount importance; a linear collider would be able to make precise determinations of the Higgs couplings to all particles (including invisible states), as well as of its total width, quantum numbers and perhaps even the strength of its self coupling. Such measurements would point the way to possible extensions of the Standard Model.

High luminosity operation would be necessary at the optimum energy for Higgs production. In this scenario, revisiting the Z pole might be critical to refine knowledge of electroweak loop corrections. Increased energy would likely be required to search for new phenomena such as strong scattering of WW pairs or evidence for large extra dimensions.

3. *No new particles are found.* This uncomfortable scenario extends the puzzlement we are in today. In this case the first goal of a linear collider would be to close the loopholes in the LHC measurements (such as the possibility that the Higgs decays dominantly to invisible particles). After that, a detailed study of the top quark or gauge boson couplings would be necessary to reveal evidence for new dynamics. In this scenario, increased energy would be necessary to study WW scattering. One might wish to carry out additional precise measurements at the Z^0 pole.
4. *A wealth of new phenomena is sighted at LEP, Tevatron and LHC.* These discoveries would indicate a much richer array of new particles and phenomena than are presently envisioned in any single model. In this case, with multiple sources of new physics, the job of the linear collider is clear. With its unparalleled ability to make detailed measurements of the properties of the new states, a linear collider would be essential to map out the terrain. A long and rich program would be assured.

In each of these representative scenarios, after examination of the many ways that new physics might come into view, we conclude that a linear collider has a decisive role to play. Starting with initial operation at 500 GeV, and continuing to higher energies as needed, an e^+e^- linear collider would be at the heart of a rich 20-year program of experimentation and discovery in high energy physics.

There is no guarantee in physics that we can ever predict how Nature chooses to operate in uncharted territory. Over the past two decades, however, through theory and experiment, a remarkable understanding has developed. In this paper we have argued that the data offer a clear picture of how the next step should proceed: We should begin the detailed design and construction of a 500 GeV e^+e^- linear collider.

ACKNOWLEDGMENTS

We are grateful to many colleagues in the US, Canada, Europe, and Japan for the insights into linear collider physics which are reflected in this document. This work was supported by grants to the authors from the US Department of Energy and the US National Science Foundation.

References

- [1] H. Murayama and M. E. Peskin, *Ann. Rev. Nucl. Part. Sci.* **46**, 533 (1996), hep-ex/9606003.
- [2] E. Accomando *et al.* [ECFA/DESY LC Physics Working Group Collaboration], *Phys. Rept.* **299**, 1 (1998), hep-ph/9705442.
- [3] S. Kuhlman *et al.* [NLC ZDR Design Group and NLC Physics Working Group Collaboration], *Physics and Technology of the Next Linear Collider: A Report Submitted to Snowmass '96*, hep-ex/9605011.
- [4] *Physics and Experiments with Future Linear e^+e^- Colliders*, E. Fernández and A. Pacheco, eds. (UAB Publications, Barcelona, 2000).
- [5] J. D. Bjorken, *Phys. Rev.* **D19**, 335 (1979).
- [6] P. Q. Hung and J. J. Sakurai, *Ann. Rev. Nucl. Part. Sci.* **31**, 375 (1981).
- [7] M. Claudson, E. Farhi and R. L. Jaffe, *Phys. Rev.* **D34**, 873 (1986).
- [8] M. Suzuki, *Phys. Rev.* **D37**, 210 (1988).
- [9] A. Sirlin, in *Proceedings of the XIX International Symposium on Lepton and Photon Interactions at High Energies*, J. A. Jaros and M. E. Peskin, eds. (World Scientific, 2000). hep-ph/9912227.
- [10] N. Bahcall, J. P. Ostriker, S. Perlmutter and P. J. Steinhardt, *Science* **284**, 1481 (1999), astro-ph/9906463.
- [11] See Chapter 4 of E. W. Kolb and M. S. Turner, *The Early Universe*. (Addison-Wesley, 1990).
- [12] Y. Fukuda *et al.* [Super-Kamiokande Collaboration], *Phys. Rev. Lett.* **81**, 1562 (1998), hep-ex/9807003.
- [13] M. Chanowitz, M. Golden and H. Georgi, *Phys. Rev. Lett.* **57**, 2344 (1986); M. S. Chanowitz, in *Proceedings of the 23rd International Conference on High Energy Physics*, S. C. Loken, ed. (World Scientific, 1987).
- [14] M. S. Chanowitz and W. Kilgore, *Phys. Lett.* **B322**, 147 (1994), hep-ph/9311336.
- [15] T. L. Barklow *et al.*, in *New Directions for High-Energy Physics: Snowmass 96*, D. G. Cassel, L. T. Gennari, and R. H. Siemann, eds. (SLAC, 1997). hep-ph/9704217.

- [16] P. Raimondi *et al.*, in Proceedings of EPAC 98, S. Myers, L. Lijebjy, Ch. Petit-Jean-Genaz, J. Poole, and K.-G. Rensfelt, eds. (IOP Publishing, 1998), SLAC-PUB-7847.
- [17] P. Chen *et al.*, in New Directions for High-Energy Physics: Snowmass 96, D. G. Cassel, L. T. Gennari, and R. H. Siemann, eds. (SLAC, 1997).
- [18] J. P. Delahaye *et al.*, Acta Phys. Polon. **B30** (1999) 2029; H. H. Braun *et al.*, CERN-99-06.
- [19] J. Irwin and R. Ruth, in preparation.
- [20] P. Raimondi and A. Seryi, SLAC-PUB-8460 (2000).
- [21] S. Weinberg, Phys. Rev. **D19**, 1277 (1979).
- [22] L. Susskind, Phys. Rev. **D20**, 2619 (1979).
- [23] K. Inoue, A. Kakuto, H. Komatsu and S. Takeshita, Prog. Theor. Phys. **68**, 927 (1982).
- [24] L. E. Ibáñez, Nucl. Phys. **B218**, 514 (1983); L. E. Ibáñez and C. López, Phys. Lett. **B126**, 54 (1983).
- [25] J. Ellis, J. S. Hagelin, D. V. Nanopoulos and K. Tamvakis, Phys. Lett. **B125**, 275 (1983).
- [26] L. Alvarez-Gaumé, J. Polchinski and M. B. Wise, Nucl. Phys. **B221**, 495 (1983).
- [27] K. D. Lane and M. E. Peskin, in Proceedings of the 15th Rencontre de Moriond, J. Tran Thanh Van, ed. (Editions Frontieres, 1980).
- [28] R. S. Chivukula, S. B. Selipsky and E. H. Simmons, Phys. Rev. Lett. **69**, 575 (1992), hep-ph/9204214;
- [29] L. Randall, Nucl. Phys. **B403**, 122 (1993), hep-ph/9210231.
- [30] R. Sundrum, Nucl. Phys. **B395**, 60 (1993), hep-ph/9205203.
- [31] T. Appelquist, J. Terning and L. C. Wijewardhana, Phys. Rev. Lett. **79**, 2767 (1997), hep-ph/9706238.
- [32] B. A. Dobrescu and C. T. Hill, Phys. Rev. Lett. **81**, 2634 (1998), hep-ph/9712319; R. S. Chivukula, B. A. Dobrescu, H. Georgi and C. T. Hill, Phys. Rev. **D59**, 075003 (1999), hep-ph/9809470.
- [33] S. Dimopoulos, S. Raby and F. Wilczek, Phys. Rev. **D24**, 1681 (1981).
- [34] M. B. Einhorn and D. R. Jones, Nucl. Phys. **B196**, 475 (1982).
- [35] L. E. Ibanez and G. G. Ross, Phys. Lett. **B105**, 439 (1981).
- [36] P. Langacker and N. Polonsky, Phys. Rev. **D47**, 4028 (1993), hep-ph/9210235, Phys. Rev. **D52**, 3081 (1995), hep-ph/9503214.
- [37] A more detailed discussion of the Higgs mass limits within the Minimal Standard Model can be found in Chapter 2.5 of J. F. Gunion, H. E. Haber, G. Kane, and S. Dawson, The Higgs Hunter’s Guide. (Addison-Wesley, 1990.)
- [38] T. Moroi and Y. Okada, Phys. Lett. **B295**, 73 (1992).

- [39] G. L. Kane, C. Kolda and J. D. Wells, Phys. Rev. Lett. **70**, 2686 (1993), hep-ph/9210242.
- [40] J. R. Espinosa and M. Quirós, Phys. Rev. Lett. **81**, 516 (1998), hep-ph/9804235.
- [41] H. E. Haber, in Proceedings of the 4th International Symposium on Radiative Corrections, hep-ph/9901365.
- [42] A. Straessner, talk presented at the XXXV Rencontres de Moriond, March 2000.
- [43] V. A. Novikov *et al.* Rept. Prog. Physics **62**, 1275 (1999).
- [44] B. Holdom and J. Terning, Phys. Lett. **B247**, 88 (1990).
- [45] M. Golden and L. Randall, Nucl. Phys. **B361**, 3 (1991).
- [46] M. E. Peskin and T. Takeuchi, Phys. Rev. Lett. **65**, 964 (1990); Phys. Rev. **D46**, 381 (1992).
- [47] M. E. Peskin and J. D. Wells, hep-ph/0101342.
- [48] R. Barbieri and G. F. Giudice, Nucl. Phys. **B306**, 63 (1988).
- [49] G. G. Ross and R. G. Roberts, Nucl. Phys. **B377**, 571 (1992).
- [50] B. de Carlos and J. A. Casas, Phys. Lett. **B309**, 320 (1993), hep-ph/9303291.
- [51] G. W. Anderson and D. J. Castaño, Phys. Rev. **D52**, 1693 (1995), hep-ph/9412322;
- [52] K. L. Chan, U. Chattopadhyay and P. Nath, Phys. Rev. **D58**, 096004 (1998), hep-ph/9710473.
- [53] L. Giusti, A. Romanino and A. Strumia, Nucl. Phys. **B550**, 3 (1999), hep-ph/9811386.
- [54] J. L. Feng, K. T. Matchev and T. Moroi, Phys. Rev. Lett. **84**, 2322 (2000), hep-ph/9908309, Phys. Rev. **D61**, 075005 (2000), hep-ph/9909334.
- [55] J. Gasser and H. Leutwyler, Nucl. Phys. **B250**, 465 (1985).
- [56] R. S. Chivukula, E. H. Simmons and J. Terning, Phys. Lett. **B331**, 383 (1994), hep-ph/9404209.
- [57] K. Hagiwara and N. Kitazawa, Phys. Rev. **D52**, 5374 (1995), hep-ph/9504332.
- [58] U. Mahanta, Phys. Rev. **D55**, 5848 (1997), hep-ph/9611289; Phys. Rev. **D56**, 402 (1997).
- [59] G. L. Kane, G. D. Kribs, S. P. Martin and J. D. Wells, Phys. Rev. **D53**, 213 (1996), hep-ph/9508265.
- [60] A. Miyamoto, in Physics and Experiments with Linear e^+e^- Colliders, F. A. Harris, S. L. Olsen, S. Pakvasa, and X. Tata, eds. (World Scientific, 1993).
- [61] Report of the Tevatron Higgs Working Group, <http://fnth37.fnal.gov/susy.html>.
- [62] ATLAS Detector and Physics Performance Technical Design Report, LHCC 99-14/15 (1999).
- [63] JLC Group, JLC-I. KEK-Report 92-16 (1992).

- [64] J. F. Gunion, H. E. Haber and J. Wudka, Phys. Rev. **D43**, 904 (1991).
- [65] D. Rainwater and D. Zeppenfeld, Phys. Rev. **D60**, 113004 (1999), hep-ph/9906218; T. Plehn, D. Rainwater and D. Zeppenfeld, Phys. Rev. **D61**, 093005 (2000), hep-ph/9911385.
- [66] M. Battaglia, in [4], hep-ph/9910271.
- [67] A. S. Kronfeld, Nucl. Phys. Proc. Suppl. **63**, 311 (1998), hep-lat/9710007.
- [68] D. L. Borden, D. A. Bauer and D. O. Caldwell, Phys. Rev. **D48**, 4018 (1993).
- [69] P. Janot, in Physics and Experiments with Linear e^+e^- Colliders, F. A. Harris, S. L. Olsen, S. Pakvasa, and X. Tata, eds. (World Scientific, 1993).
- [70] B. Grzadkowski and J. F. Gunion, Phys. Lett. **B294**, 361 (1992), hep-ph/9206262.
- [71] E. Asakawa, J. Kamoshita, A. Sugamoto and I. Watanabe, Eur. Phys. J. **C14**, 335 (2000), hep-ph/9912373.
- [72] A. Djouadi *et al.* hep-ph/9904287.
- [73] A. Djouadi *et al.* hep-ph/9903229.
- [74] M. E. Peskin, Prog. Theor. Phys. Suppl. **123**, 507 (1996), hep-ph/9604339.
- [75] S. Abdullin *et al.* [CMS Collaboration], hep-ph/9806366.
- [76] N. Danielson, http://hep-www.colorado.edu/SUSY/danielson_thesis.ps.
- [77] H. Martyn and G. A. Blair, in [4], hep-ph/9910416.
- [78] M. N. Danielson, *et al.*, in New Directions for High-Energy Physics: Snowmass 96, D. G. Cassel, L. T. Gennari, and R. H. Siemann, eds. (SLAC, 1997).
- [79] T. Tsukamoto, K. Fujii, H. Murayama, M. Yamaguchi and Y. Okada, Phys. Rev. **D51**, 3153 (1995).
- [80] M. M. Nojiri, K. Fujii and T. Tsukamoto, Phys. Rev. **D54**, 6756 (1996), hep-ph/9606370.
- [81] H. Cheng, J. L. Feng and N. Polonsky, Phys. Rev. **D56**, 6875 (1997), hep-ph/9706438, Phys. Rev. **D57**, 152 (1998), hep-ph/9706476.
- [82] M. M. Nojiri, D. M. Pierce and Y. Yamada, Phys. Rev. **D57**, 1539 (1998), hep-ph/9707244; S. Kiyoura, M. M. Nojiri, D. M. Pierce and Y. Yamada, Phys. Rev. **D58**, 075002 (1998), hep-ph/9803210.
- [83] E. Katz, L. Randall and S. Su, Nucl. Phys. **B536**, 3 (1998), hep-ph/9801416.
- [84] Y. Kato, in [4], hep-ph/9910293.
- [85] J. L. Feng, M. E. Peskin, H. Murayama and X. Tata, Phys. Rev. **D52**, 1418 (1995), hep-ph/9502260.
- [86] J. L. Feng and M. J. Strassler, Phys. Rev. **D51**, 4661 (1995), hep-ph/9408359; Phys. Rev. **D55**, 1326 (1997), hep-ph/9606477.

- [87] R. Frey *et al.*, in *New Directions for High-Energy Physics: Snowmass 96*, D. G. Cassel, L. T. Gennari, and R. H. Siemann, eds. (SLAC, 1997), hep-ph/9704243.
- [88] *Future Electroweak Physics at the Fermilab Tevatron*, D. Amidei and R. Brock, eds. FERMILAB-PUB-96/082.
- [89] Y. Sumino, *Acta Phys. Polon.* **B25**, 1837 (1994), hep-ph/9411310.
- [90] A. H. Hoang, *Nucl. Phys. Proc. Suppl.* **86**, 512 (2000), hep-ph/9909356.
- [91] A. H. Hoang *et al.*, *Eur. Phys. J. direct* **C3**, 1 (2000), hep-ph/0001286.
- [92] K. Fujii, T. Matsui, and Y. Sumino, *Phys. Rev.* **D50**, 4341 (1994).
- [93] P. Comas, R. Miquel, M. Martinez, and S. Orteu, in *Physics and Experiments with Linear Colliders*, A. Miyamoto, Y. Fujii, and T. Matsui, eds. (World Scientific, 1996).
- [94] D. Peralta, M. Martinez, and R. Miquel, in [4].
- [95] B. Grzadkowski and Z. Hioki, *Phys. Lett.* **B476**, 87 (2000), hep-ph/9911505, hep-ph/0004223.
- [96] T. G. Rizzo, hep-ph/9605361.
- [97] T. L. Barklow and C. R. Schmidt, in *The Albuquerque Meeting (DPF94)*, S. Seidel, ed. (World Scientific, 1995).
- [98] H. Baer, S. Dawson and L. Reina, *Phys. Rev.* **D61**, 013002 (2000), hep-ph/9906419.
- [99] A. Juste and G. Merino, hep-ph/9910301.
- [100] J. Ellison and J. Wudka, *Ann. Rev. Nucl. Part. Sci.* **48**, 33 (1998).
- [101] G. Bella *et al.* [LEP TGC Working Group], LEPEWWG/TGC/2000-01, (March 2000).
- [102] E.N. Argyres *et al.*, *Nucl. Phys.* **B391**, 23 (1993).
- [103] B. Abbott *et al.* (DØ Collaboration), *Phys. Rev.* **D60**, 072002 (1999).
- [104] S. Haywood *et al.*, hep-ph/0003275, to appear in the CERN Yellow Report on “Standard Model Physics (and More) at the LHC”.
- [105] C. Burgard, in [4].
- [106] P. N. Burrows *et al.*, in *New Directions for High-Energy Physics: Snowmass 96*, D. G. Cassel, L. T. Gennari, and R. H. Siemann, eds. (SLAC, 1997), hep-ex/9612012. B. A. Schumm, hep-ex/9612013
- [107] S. J. Brodsky, F. Hautmann and D. E. Soper, *Phys. Rev.* **D56**, 6957 (1997), hep-ph/9706427.
- [108] R. Hawkings and K. Monig, hep-ex/9910022. J. Erler, S. Heinemeyer, W. Hollik, G. Weiglein and P. M. Zerwas, hep-ph/0005024.
- [109] V. Ruhlmann-Kleider, in *Proceedings of the XIX International Symposium on Lepton and Photon Interactions at High Energies*, J. A. Jaros and M. E. Peskin, eds. (World Scientific, 2000). hep-ex/0001061.

- [110] E. Boos, H. J. He, W. Kilian, A. Pukhov, C. P. Yuan and P. M. Zerwas, Phys. Rev. **D57**, 1553 (1998), hep-ph/9708310; Phys. Rev. **D61**, 077901 (2000), hep-ph/9908409.
- [111] T. Han, Y. J. Kim, A. Likhoded and G. Valencia, hep-ph/0005306.
- [112] J. L. Feng and T. Moroi, Phys. Rev. **D56**, 5962 (1997), hep-ph/9612333.
- [113] J. L. Feng and D. E. Finnell, Phys. Rev. **D49**, 2369 (1994), hep-ph/9310211.
- [114] A. Bartl, H. Eberl, S. Kraml, W. Majerotto and W. Porod, hep-ph/0002115.
- [115] P. M. Zerwas, hep-ph/0003221; G. A. Blair, W. Porod and P. M. Zerwas, Phys. Rev. D **63**, 017703 (2001), hep-ph/0007107.
- [116] J. L. Hewett and T. G. Rizzo, Phys. Rept. **183**, 193 (1989).
- [117] A. Leike, Phys. Rept. **317**, 143 (1999), hep-ph/9805494.
- [118] M. Cvetič and P. Langacker, hep-ph/9707451.
- [119] M. Cvetič and P. Langacker, Mod. Phys. Lett. **A11**, 1247 (1996), hep-ph/9602424.
- [120] A. Leike and S. Riemann, hep-ph/9604321.
- [121] M. Cvetič and S. Godfrey, hep-ph/9504216.
- [122] F. Del Aguila, M. Cvetič and P. Langacker, Phys. Rev. **D52**, 37 (1995), hep-ph/9501390.
- [123] T. G. Rizzo, Int. J. Mod. Phys. **A13**, 2245 (1998), hep-ph/9710229.
- [124] T. L. Barklow, Int. J. Mod. Phys. **A11**, 1579 (1996).
- [125] I. Antoniadis, Phys. Lett. **B246**, 377 (1990).
- [126] J. D. Lykken, Phys. Rev. **D54**, 3693 (1996), hep-th/9603133.
- [127] N. Arkani-Hamed, S. Dimopoulos and G. Dvali, Phys. Lett. **B429**, 263 (1998), hep-ph/9803315.
- [128] M. E. Peskin, hep-ph/0002041, to appear in the Proceedings of the 1999 European Physical Society High Energy Physics Conference.
- [129] L. Randall and R. Sundrum, Phys. Rev. Lett. **83**, 3370 (1999), hep-ph/9905221.
- [130] H. Davoudiasl, J. L. Hewett and T. G. Rizzo, Phys. Rev. Lett. **84**, 2080 (2000), hep-ph/9909255, hep-ph/0006041.
- [131] ALEPH Collaboration, ALEPH 99-051, paper contributed to the 1999 European Physical Society High Energy Physics Conference.
- [132] M. Acciarri *et al.* [L3 Collaboration], Phys. Lett. **B470**, 281 (1999), hep-ex/9910056.
- [133] G. Landsberg [DØ Collaboration], presentation at the April, 2000, APS meeting.
- [134] J. L. Hewett, in [4].

